Environmental Modelling and Software 145 (2021) 105204

Contents lists available at ScienceDirect

Environmental Modelling and Software

journal homepage: www.elsevier.com/locate/envsoft

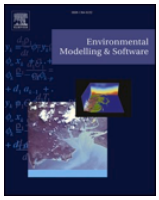

India's Maiden air quality forecasting framework for megacities of divergent environments: The SAFAR-project

Gufran Beig [a,*], S.K. Sahu [b], V. Anand [a,c], S. Bano [a], S. Maji [a], A. Rathod [a], N. Korhale [a,c], S. B. Sobhana [a], N. Parkhi [a], P. Mangaraj [b], R. Srinivas [a], S.K. Peshin [d], S. Singh [d], R. Shinde [a], H. K. Trimbake [a]

[a] Indian Institute of Tropical Meteorology, Pune, Ministry of Earth Sciences, India
[b] Utkal University, Bhubaneshwar, India
[c] Savitribai Phule Pune University, Pune, India
[d] Indian Meteorological Department, New Delhi, India

ARTICLE INFO

Keywords:
Particulate matters
Air quality
SAFAR
Meteorology
Forecasting model
Megacities
Environment
Topography and health

ABSTRACT

Air quality is a strong health driver, its accurate assessment and forecast are important in densely populated megacities to take preventive steps. We describe the first Indian operational air quality framework, SAFAR (System of Air Quality and Weather Forecasting And Research), meant for decision-makers and a research tool with a capability of three days advance forecast in four Indian megacities of distinct environment and topography. The framework includes six different components from observations and modelling to outreach. To evaluate the performance of the forecast, we focus on particulate pollutants which largely define air quality of Indian metropolis. The model prediction skill is tested for the pilot year 2019-20 which is found to be reasonable. The Normalized Gross error of $PM_{2.5}$ for Delhi is found to be highest (35%) whereas for other cities it is ~13–20%. The Model Output Statistics (MOS) application enhanced operational forecast ability of numerical model which resulted in improving the accuracy for specific seasons (winter).

1. Introduction

During past few decades human activities have changed the chemical composition of the atmosphere considerably at a local, regional and global level causing several problems of global concern, air pollution, global warming, climate change, are a few of them. The problem of air pollution has become serious in Indian metropolitan cities. After the economic liberalization, India has become one of the world's fastest-growing economies. The economic and social development in India has been reflected in the rapidly growing industrialization, urbanization, increased transportation, etc. which on the other hand also contributed in increasing the emissions of air pollutants. High levels of particulate matter concentrations impact human health (Balakrishnan et al., 2019) and affect the radiative balance through direct and indirect effects (Seinfeld and Pandis, 2006). Exposure to $PM_{2.5}$ for prolonged periods can lead to serious health effects such as decreased lung function, chronic bronchitis, and premature mortality (US EPA, 2005, 2019). Ground-level ultra-fine particulate matter $PM_{2.5}$ (particles having aerodynamic diameter $\leq$2.5 μm) is the major concern in Indian urban complexes and hence National Ambient Air Quality Standards (NAAQS) have been set up for such pollutants in India like by many other countries throughout the world. The level of $PM_{2.5}$ routinely exceeds the 24-h standard of 60 μgm^{-3} established by the Indian Government (MoEFCC, 2015).

Pollution is largely added to the atmosphere by surface emissions from various sources including anthropogenic and natural emissions. In addition to the emissions, meteorological processes on various spatial and temporal scales strongly affect air quality. The air quality may be affected by distance transport (long to short-range) and local weather. Meteorological factors that may affect PM include temperature, wind speed, wind direction, relative humidity (RH), high-pressure system, mixing height, ventilation coefficient and atmospheric stability. Extreme weather events such as heatwaves, droughts, and air stagnation are particularly important when air pollutants accumulate over a relatively long time period during the event. Summer monsoon is an important feature for India and modulates the air quality. Through

* Corresponding author.
E-mail address: beig@tropmet.res.in (G. Beig).

https://doi.org/10.1016/j.envsoft.2021.105204
Accepted 11 September 2021
Available online 15 September 2021

Graphic Abstract

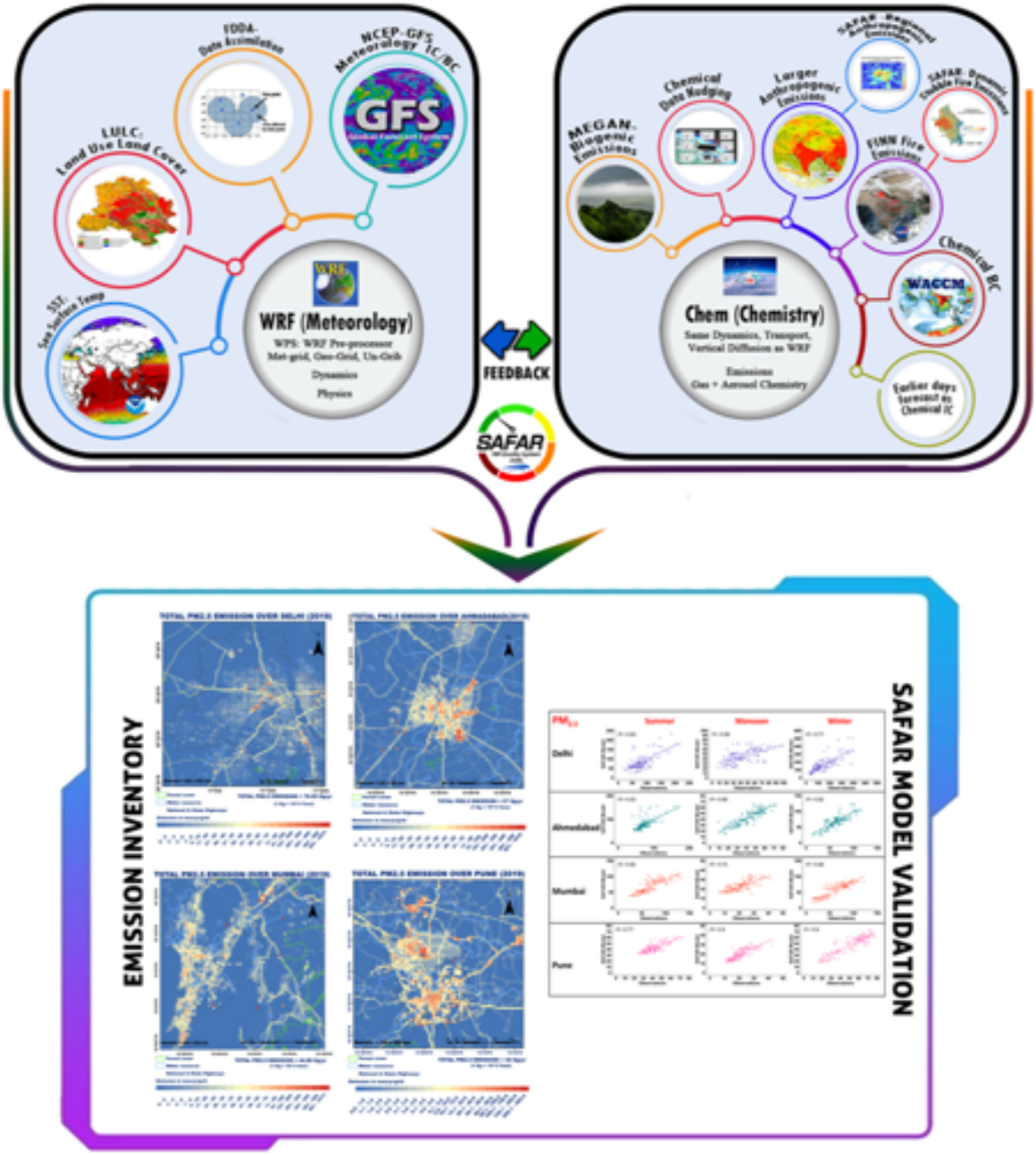

various weather processes, climate change may directly affect air quality by modulating emission inventories and dispersion patterns. Understanding the impact of weather on air quality in a changing climate is extremely important as a prerequisite to any prediction system.

Environmental monitoring and early warning system are the basics of long-term development of environmental protection work. To improve the quality of people's health and life, the development of a robust, accurate and simple air quality monitoring and early warning system is highly desirable. Such a system is also essential to effectively fulfil the requirement of a decision support system which includes various components from observations and predictive capabilities to disseminating strategy at a city level. Air quality event information in advance can assist the general public in coping with health and environmental problems and take more efficient counter measures (Schell et al., 2001). Air quality problem and forecasting capability is developed by quite a few developed countries but such systems are sparse in the developing world.

When India hosted the 19th Commonwealth Games in 2010, a need was felt to provide the air quality and weather information to around 8000 athletes from 71 commonwealth nations in Indian capital megacity Delhi as the air pollution is known to impact the performance of athletes (Shephard, 1984). Several controlled studies with athletes have shown that exercise while breathing elevated levels of air pollution which may have a direct impact on athletic performance (Rundell, 2012). In order to address the pressing need and to provide better tools for decision-makers, the Indian air quality forecasting framework, known as SAFAR (System of Air Quality and Weather Forecasting and Research) has been developed for Indian megacities. SAFAR is the Indian Government's first official operational air quality forecasting framework successfully conceived, designed and developed by Indian Institute of Tropical Meteorology Pune, a constituent of Indian Ministry of Earth Sciences. The SAFAR project is also adopted as a pilot study of GURME, World Meteorological Organization (Beig et al., 2015). The SAFAR is an early warning framework designed with an objective to predict air quality 3 days in advance along with weather parameters and translate data into information for the benefit to the society. After the successful demonstration of SAFAR project in Delhi, its usefulness to the common public and society became evident. Thereafter, Indian government, decided to further expand it in three more major cities of India, namely, Pune, Mumbai and Ahmedabad. In addition to understanding the scientific processes governing the day-to-day variability of air quality and weather parameters, SAFAR connects scientific outcome with society to increase preparedness amongst common citizens and help decision makers to reduce health risk associated with air pollution hazards. Since each of the four megacities represent a distinct micro-environment and climatology, it provided a challenge to forecasting models and an opportunity to understand different processes controlling the air quality in different environments. The operational online chemistry-transport-model (CTMs) with forecasting applications to multiple Indian cities of different micro-climate was non-existent in India until SAFAR was conceived. This is mainly due to many difficulties; major among them is the deficiency in the gridded emission inventory in absence of micro-level activity data (Sahu et al., 2011). In addition to this, difficulties also arise in simulating meteorological fields over an area of complex geography, with significant variabilities in weather parameters among different cities.

The objective of the current paper is to discuss the strategic framework of SAFAR development which includes different components consisting of monitoring network, emissions, modelling (forecasting) and its validation, and communication. The CTMs which are deterministic models can forecast air pollution concentrations but the accuracy of the forecast is highly affected by the quality of the emission data and the scale used, the incomplete knowledge on the sources, transport processes and atmospheric chemicals (Vara-Vela et al., 2016) which have also been addressed in this paper. To evaluate the forecasting performance of the SAFAR model, we have applied various statistical metrics. The Model Output Statistics (MOS) is a type of statistical post-processing, a class of techniques used to improve numerical models' ability to forecast (Glahn and Lowry, 1972; Carter et al., 1989). Many forecasting systems around the globe apply the MOS application to improve the operational forecasting. Perez et al. (2015) developed the MOS algorithm to enhance the air quality forecast in Spain. Impact of data stratification on the efficiency of the MOS methodology to a high-resolution deterministic air quality forecast in Poland is reported by Struzewska et al. (2016). A comprehensive discussion on improving the atmospheric Chemistry forecast using MOS application is provided by Ma et al. (2018) and references therein. The SAFAR framework also includes the MOS application to test and improve the skill of air quality forecast. The translating of the scientific data to information and its effective dissemination is a key to any air quality management system which is also addressed within SAFAR-framework.

2. Climatology of study region

Fig. 1 shows the zoomed map of four Indian megacities of India having distinct topography and micro-climate (Anand et al., 2019). The location of India in the global map is also depicted in Fig. 1. The major roads, highways, water resource, forest cover, build-up land, agriculture land, slum areas, power plants and industrial locations are marked in each city map. Delhi is officially known as the National Capital Territory (NCT), it is a megacity of India containing New Delhi, the capital of India situated in the country's North at 28.61°N 77.23°E. While, the whole NCT's population was about 17 million; Delhi's urban area is now considered to extend beyond the NCT boundaries, and include the neighboring satellite cities of Ghaziabad, Faridabad, Gurgaon and Noida in an area called the National Capital Region (NCR) and had an estimated 2016 population of over 26 million people, making it the world's second-largest urban area according to the United Nations (UN report, 2016). Geographically, Delhi is a landlocked city that experiences very hot summers and severe winters and is located at an elevation of 216 m above sea level to cover an area of 1484 sq. km. The temperature may rise to about 47 °C in summers and go down to about 2 °C in winter. The monsoon starts in late June and lasts until mid-September with an average annual rainfall of approximately 886 mm. Winters are influenced by the Western disturbances and cold winds from the Himalayas making the winters chilly. Due to the proximity to the Arabian Sea, Mumbai has humid weather. During monsoon season, Mumbai witnesses heavy rainfall. Mumbai is at an elevation of about 14 m.

above sea level and has a population of 12 million. Temperatures do not vary much throughout the year and it remains between 32 °C and 40 °C. Humidity is highest during the summer months and it records rainfall of 1800 mm. The winds from the western side are the most noticeable feature of Mumbai monsoons. Pune is located in the Western Ghats of Sahyadri mountain range. It is about 100 km inland from the western coast of India at 559 m above mean sea level with a population of approximately 9 million. The climate of Pune is mainly dry with a low-latitude semi-arid hot climate. The city receives an annual rainfall of 722 mm, mainly between June and September as a result of the south-west monsoon. Ahmedabad which is a city in the western state of Gujarat has a tropical semiarid climate. It is located at an elevation of about 53 m above mean sea level having a population of over 5 million. The annual rainfall is about 700 mm. This city experiences severe summers with temperatures varying between 24 °C and 50 °C. Winters are not very severe here and the temperature does not fall significantly. In this study, the seasonal variability in the particulate matter levels is considered by taking into account three major seasons, namely, Summer (February, March, April & May), Monsoon (June, July, August, September) and winter (October, November, December, January) as per the observed climatology of tropical North-Western cities of India (Anand et al., 2019).

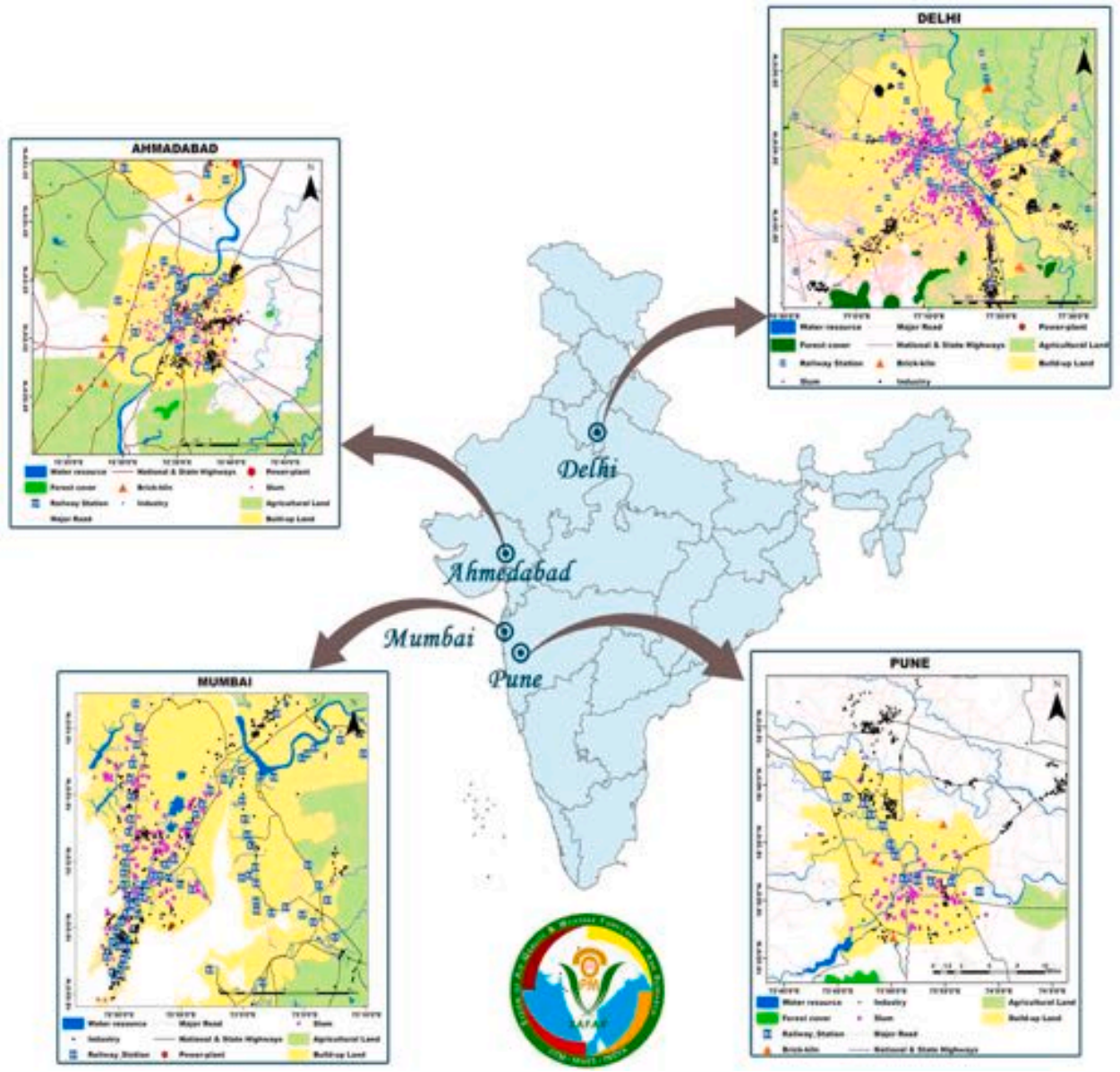

Fig. 1. The location map of four Indian megacities with classification of different topographic parameters are zoomed from Indian map. The SAFAR framework is developed in these 4 cities namely, Delhi, Ahmedabad, Mumbai and Pune. The location of India is also shown on the world map.

3. SAFAR framework design and implementation

This section introduces the strategic framework of SAFAR and its interdisciplinary approach. The process of developing such a framework is complex and involves round the clock measurements of various air quality and weather parameters, analyzing the same with basic scientific knowledge, improving forecasting capabilities with basic scientific research, translating science to information products and disseminating the information in very simple and user friendly format so that maximum stakeholders including government agencies, educational institutes, common public can understand and use the same for their benefit ranging from safeguarding health to mitigation measures. The data dissemination in an easy to understand format is ensured by adapting modern communication techniques. The SAFAR framework consists of six different components and integrates them.

1. *Observational Network*: Air Pollutants and Weather Parameters
2. *Quality Assurance and Quality Control* (QA-QC): Above parameters
3. *Emission Inventory*: For accounting sources of pollutants.
4. *SAFAR-Forecasting Model*: Establishment of high-resolution air quality forecasting model.
5. *Translating Data to Information*: Concept of AQI
6. *Technological Framework and Outreach:* Data management, product generation, and Dissemination

The SAFAR data communication framework is shown in Figure- 2. It has two components, namely, the remote data transfer and master control centre. All servers located in master control centre are connected physically with high-speed internet lines. The near real time online raw data of different pollutants along with weather parameters measured at various stations located in different locations of a city first saved in the data logger connected physically at each Air Quality Monitoring Station (AQMS) represented as “monitoring” in the right side of Fig. 2. Once stored locally, data get transferred remotely through GPRS/4G/5G network in to data server located at Master Control center. The SAFAR atmospheric Chemistry transport model runs at supercomputer which is located in a different location within the campus and represented as “Modelling” in the left side of Fig. 2. The model output of desired

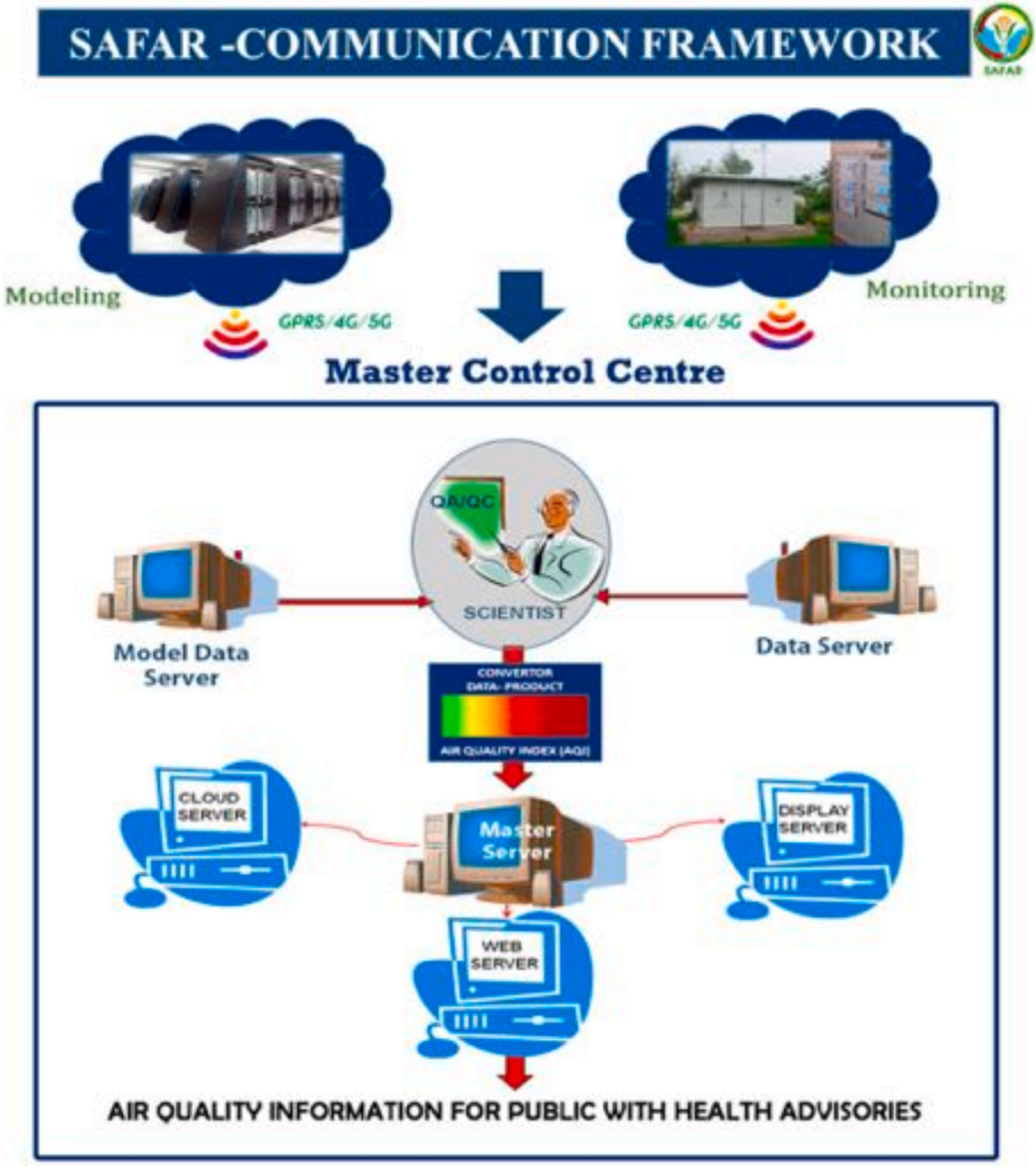

Fig. 2. A flow diagram of data communication and dissemination of SAFAR framework.

forecast data is remotely transferred to model data server located in the master control center. Now onwards all the functions are done in master control center. Both sets of data consisting of current and forecasted air quality and weather parameters. The data is then checked for quality assurance and quality control (QA-QC) as per protocol by expert operational team. The MOS application is applied here. Then the data is passed on to FTP Master Server. The algorithm loaded at FTP master server converts this data received in physical units into Indian national Air Quality Index (AQI) and other related parameters in easy-to-understand format. SAFAR products are generated and stored at FTP master server which has the responsibility to channel the data to various disseminating servers like display server, WEB server and cloud servers from where the system products get disseminated to the society via wireless communication network. We will discuss each component of SAFAR framework in the subsequent sub-section below.

3.1. Observations network

The SAFAR framework consists of more than 40 monitoring stations in four SAFAR cities, with nearly 100, monitoring instruments. Each city network includes 10 Air Quality Monitoring Stations (AQMS) which have online analysers that are US-EPA approved, distributed in different microenvironments viz. downtown area, background, industrialized area, residential area, traffic areas, etc. in such a way that they cover the

whole city and the average can be representative of the city as per WMO guidelines (Grimmond et al., 2014; Srinivas et al., 2016; Beig et al., 2015). The Automatic Weather Stations (AWS) to measure different meteorological parameters are collocated with each AQMS. Observational network in the urban complex is required to get near real time air quality and weather data over the strategic locations which can be then used for improving forecast and its validation. Urban areas are complex and shows variation at micro-scale. WMO has set up standard guidelines to establish air quality and weather monitoring stations in urban areas (WMO, 2008, 2014; Grimmond et al., 2014) which get updated from time to time. As per the guidelines, strategic selection of monitoring stations and their density is needed, based on the range of applications and the nature of the variability of the city. To develop a forecast system for air quality and weather, stations should cover all kinds of land uses (e.g., highly dense urban, residential, industrial, suburban), catchments, downwind and upwind areas so that it could be representative of an urban cluster/megacity (Bieringer et al., 2013; Grimmond et al., 2014) which has been adopted in this work. Selecting the density of monitoring station can be decided based on the availability of resources. In addition to the installation of instruments to find out prevailing surface characteristics, SAFAR framework adopts Standard Operating Procedure (SOP) for robust quality control/quality check (QA-QC) to ensure good data quality which is discussed in subsequent section.

The air quality indicators and weather parameters are monitored round the clock. The data is recorded and stored at every 5 min interval at local station. Air Quality observation includes many parameters including PM10, PM2.5, on which current work is focussed. The measurements of fine particulate matter ($PM_{2.5}$) in micrograms per cubic meter ($\mu g/m^3$) were carried out with the help of Beta Attenuation Monitor (BAM-1020) during the study period. In BAM-1020, carbon-14 (^{14}C) element is used as a radioactive source which gives a constant source of high energy electrons are well known as beta rays and these particles are detected and counted by a scintillation detector. Low energy beta rays are absorbed by collision with electrons, whose number is proportional to the density. Therefore, absorption is a function of the mass of the irradiated material. The external pump pulls a measured amount of air sample (dust-laden). Afterwards, the filter tape weighed down with dust is automatically placed between the source and the detector. The attenuation of the beta particle signal is used to determine the mass concentration of aerosols collected on the filter tape. The extensive details of the BAM 1020 are reported in our previous studies (Beig et al., 2020a; Yadav et al., 2017). BAM-1020 measures the mass concentration of particulate matters which can measure up to 10,000 $\mu g/m^3$ with a lower detection limit of ~1 $\mu g/m^3$. The span calibration of the instrument is automatically verified on an hourly basis (Anand et al., 2019; Yadav et al., 2019). The data has been collected for one year during 2019-20 covering all seasons and the 24 h mean of $PM_{2.5}$ has been computed. The meteorological parameters such as wind speed (km hr^{-1}), relative humidity (%) and temperature (°C) have been measured using the automatic Weather Stations (Anand et al., 2019). This near real time online raw data is then transferred to central AQMS server at SAFAR-Control centre remotely at every 15 min interval which is a central data base where data has been validated by expert scientific team (Fig. 2). The data is subsequently averaged to 1-h interval.

3.2. Quality assurance and quality control (QA-QC)

Quality control and quality assurance (QA-QC) is the major and essential step in the operational SAFAR early warning framework, not only in monitoring instruments but also at each step. This need to be performed rigorously before disseminating data. The instruments are maintained and operated according to the standard specifications of supplier. All air quality and weather monitors need to be operated continuously (24 × 7 hr). For the purpose, following operational protocol has been developed to ensure QA-QC:

(a) Based on drift specification, instrument environment and other factors, the calibration is done at definite time interval for all the analyzers and sensors. A software will record and store data at every 5 min interval at local station with wired connectivity in data acquisition system.
(b) Near real time online raw data get transferred from respective AQMS stations to central AQMS server remotely at every 15 min interval which will act as a central data base.
(c) As part of QA-QC, we developed an SOP at central AQMS server to give alert for (1) instrument failure at site, (2) communication failure between instrument and local server and (3) communication failure between local server and central AQMS server. This SOP is adopted to prevent data loss and solve the problems with minimum time lag.
(d) The data validation is an essential function of technical management. At SAFAR-Control room, errors or suspicious data which are flagged by the system is checked and corrected by expert scientific team. Various quality codes are set to observational values based on information relating to the state of the sensor or measurement. The invalid or out of range data is carefully checked and if found spurious it is discarded for subsequent analysis. After validation, the data is subsequently averaged to 1 h/24 h/8 h based on type of pollutant and AQI formulation requirement on rolling average basis for each hour.
(e) *Technical review and audit:* Review and audit is an integral part of the system. Field engineers visit the stations on daily basis and perform check to ensure the instruments are working properly. Field engineers are responsible for reporting the daily status of instrument health to control and command centre. On monthly basis review meeting is conducted and monthly audits are performed in which instrument health as well as documentation has been checked by internal auditors consist of SAFAR scientific team members.

3.3. Emission inventory

Emission inventory is a key factor in determining the accuracy of air quality modelling results (Gao et al., 2016). It is a fundamental tool to identify all sources of pollutants and its magnitude during a particular time and geographic region, which requires both primary activity data collected from field surveys as well as secondary activity data collected from various authentic sources. Activity data is defined as the quantitative measure of the activity that results in the emissions of air pollutants. Different kinds of activities are related to a particular source of emission whose extend and intensity determines the strength of emission and it varies from place to place. Hence, there is a need to identify different activities going on in the region which are responsible for the emission of varieties of air pollutants and find out the intensity of those to be able to quantify the emissions. To make the present inventory more accurate and robust a large number of site-specific primary data has been generated and at the same time all available secondary data sets have been collected from all possible authentic sources for the selected air pollution sources in the region. The gridded emission inventory for these 4 SAFAR cities has been developed recently by us and methodology is reported in detail elsewhere (Beig et al., 2018, 2019; Sahu et al., 2011) and hence only briefly discussed in this paper. Building out a technological emission inventory involves various distinctive major and minor sources of emission. During the development of such inventory, the first step includes the recognition of each source and the second step consists of the distribution of emission geographically in grids. A bottom-up approach has been taken to develop a high-resolution gridded emission inventory with the well-established methodology discussed earlier (Sahu et al., 2015). Then the generated data are applied to country-specific technological emission factors to estimate the total emission (Beig et al., 2018; Huang et al., 2018; Filonchyk and Hurynovich 2020; Sahu et al., 2011, 2015, 2017). The activity data for 16

major/minor sectors are targeted which was rearranged into six major categories, namely, Transport, Power, Industry, Residential, Windblown dust (re-suspended dust) and rest others (includes many unattended sources like brick kiln, crematorium, etc).

An emission factor (EFs) is a representative value that attempts to relate the quantity of a pollutant released to the atmosphere with a particular activity associated with the release of that pollutant. Typically, EFs of a fuel depends on the chemical composition of the fuel, combustion type, temperature and efficiency of any emission control device. There are very limited measured EFs available in the literature for India. Incorporating a country-specific appropriate EF is a very sensitive part in the development of emission inventory. EF defines the source strength as emission per unit time and per unit activity of the process. The emission factors based on the technological fuel type have been used to estimate bottom-up emissions from each sector. A Geographic Information System (GIS) organises air quality data from a variety of sources in a uniform framework which will not only improve accuracy but also play vital role in data management. The emission values from different sources are also organized as a set of thematic layers where the GIS-based statistical methodology is adopted to prepare gridded emission inventories of particulate matter $PM_{2.5}$ and PM_{10} with 1.67 km resolution.

Uncertainty in Emission Inventory: Emission inventory is an important input to the air quality forecasting model and hence accuracy of air quality forecast depends on the reliability of emission calculations performed in the emission inventory development. In this case, it is necessary to identify and estimate uncertainties associated with emission inventories to help modelers to consider the factor while running the forecast models. Estimating the uncertainty of an emission value is often a more difficult task than estimating the emission value (Placet et al., 2000). Quantifying the uncertainties is not an easy task as it requires continuous monitoring of emissions at the source point which is not practical in real conditions. Till date, no such systematic approach for the identification of uncertainty is available. As a result, the calculated emissions cannot be exactly validated, however, uncertainties associated with the estimation can roughly be considered. Following are the factors which account for uncertainty in the emission estimates:

1) Emission factors, 2) Activity data, 3) Spatial distribution of emission, 4) Source category specification, 5) Missing data leads to approximation, 6) Poor understanding of emitting processes, 7) Uncertainty in efficiency of control equipment's, 8) Reporting error, 9) Inaccuracy in gridding process, 10) Geographical data to allocate emission, etc.

Most of occasion there is a considerable uncertainty introduced during inventory development process. Uncertainty in emission inventory is a function of the uncertainty in input data, mainly related to activity data (both primary & secondary) and emission factors. A Monte Carlo analysis is widely used for detailed category-by-category assessment of uncertainty, particularly where uncertainties are not distributed normally. Present uncertainty analysis is done by incorporating the above mentioned two critical factors. In the present work, an attempt has been made to collect city specific micro-level activity data to reduce uncertainties associated with the data; however, missing data can lead to certain assumptions and also dependency on available secondary data for certain sectors may lead to uncertainty in the present work. Monte Carlo analysis can be performed at the category level, for aggregations of categories or for the inventory as a whole. Calculation of error propagation is done by critically following the step and by accommodating different past studies for a better comparison and accuracy in analysis; the past studies (Smith et al., 2000; Gurjar et al., 2004; Arora et al., 2014) are taken into account. Combined uncertainty is calculated by considering both the emission factor as well as activity data uncertainty. The process then repeated for sectoral emissions for different years and the differences between these for the total and any sectors of interest. We have adopted region-specific emission factors variability in processes producing emissions, variation in environmental factors (e.g. temperature, humidity etc.), methods and assumptions used to fill in knowledge gaps about emissions processes and estimated the error of the order of around ±25–30%. Windblown road dust being exceptional concerning particulate matter emission only and is one of the vital contributors to the particulate matter emission having an uncertainty of ±30–41%. For rest of the pollutants the domestic source which comprises of several fuels including LPG, wood, kerosene and cow-dung i.e., residential sector shows the largest uncertainty with maximum being ±15–25%. The activity data collected through field campaign is vital in reducing the uncertainty. The most complicated uncertainty estimation calculation was for the transport sector as it involves fuel specific vehicles category, which have emission factors according to the age of vehicles. Hence calculating the uncertainty percentage for emission factor involved critical review of older studies as well. The maximum uncertainty estimated for transport sector was ±20–35%. Later accompanies the industrial and power plant sector with uncertainty of ±25–32% individually. The other sector which comprises of several minor sources showed an uncertainty of ±22–45%. It is pertinent to mention here that the magnitude of the uncertainty in found to be much higher in majority of the earlier work (Saikawa et al., 2017).

3.4. SAFAR -air quality forecasting model

Numerous types of models are available for meteorological and chemical transport modelling. These models can be configured according to the desired specifications. Several models can be combined together for better forecasting and analysis. The WRF-Chem is the most widely used community mesoscale numerical weather model in which a meteorological module is coupled on-line with a chemistry module (Grell et al., 2005). This chemistry module consists of various gaseous, aerosol, and aqueous chemistry processes to represent atmospheric chemistry occurring in the troposphere and stratosphere (Andrade et al., 2015). Being a community model, different chemistry modules get updated as more and more validation studies are conducted. WRF-Chem features two dynamical cores, a data assimilation system, and a software architecture facilitating parallel computation and system extensibility. The model serves a wide range of meteorological applications across scales from tens of meters to thousands of kilometres. WRF offers a flexible and computationally-efficient platform for operational forecasting while providing advances in physics, numeric, and data assimilation contributed by developers in the broader research community.

The chemistry of chemical species is fully coupled with the dynamical calculations in the model so that the transport scheme, emissions, mixing, horizontal and vertical grids, chemical transformation of trace gases, aerosols and the physics schemes for subgrid-scale transport are the same for both meteorological and chemical components at each time step. The Indian SAFAR forecasting framework discussed in this work is based on WRF-Chem (Weather Research and Forecast with Chemistry model version 3.9) (Powers et al., 2017; Grell et al., 2005) which provides three-day forecasts for important pollutants in Delhi, Ahmedabad, Mumbai and Pune. SAFAR framework is conceived based on the following three fundamental key components which largely govern the air quality in Indian megacities, namely (1) local emissions, (2) local weather and (3) long to short range transport with distance weather. In addition, when occasional episodic extreme external pumping coincides with favourable weather, it leads to environmental emergency. Dust storm, stubble burning, huge forest fire falls under episodic external sources. All 3 basic processes are highly coupled with each other and status of air quality cannot be understood in isolation by ignoring one over other. A schematic flow diagram for SAFAR air quality forecasting model for Indian metropolis is shown in Fig. 3 where components of meteorology and chemistry are shown in 2 independent boxes under the heading "WRF" and "CHEM" respectively in Fig. 3. This modelling framework uses a combination of meteorological fields, topography data, land use-land cover data, initial and lateral boundary conditions and emission module, etc., as shown at both ends of Fig. 3. The spatial

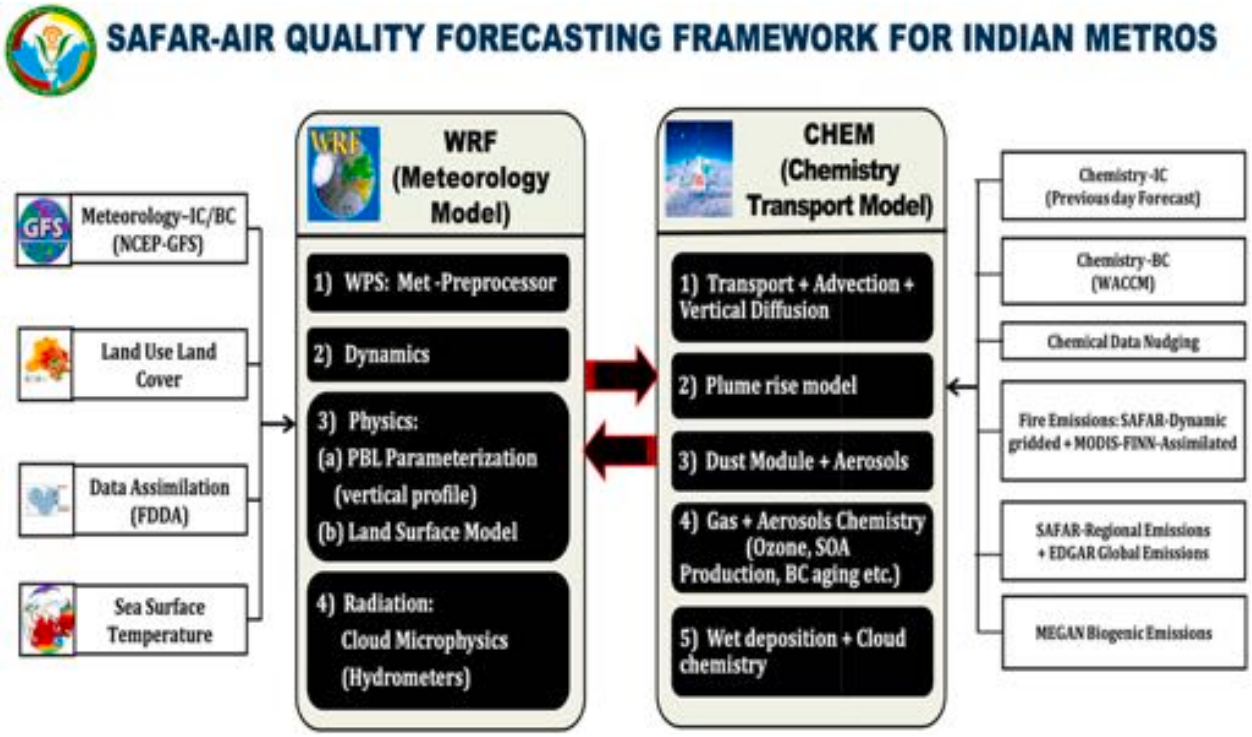

Fig. 3. Schematics of SAFAR-Air quality forecasting framework developed for the four Indian metropolitan cities based on WRF-Chem where different components of interactive meteorology and chemistry modules are shown.

representation of emission at city scale (1.67 km) was built using the detailed activity data and emission factors using bottom-up approach, to construct the gridded emission inventory (Beig et al., 2018, 2020b; Sahu et al., 2011) discussed in the previous section. The results for online simulation for the period from February 1, 2019 to January 31, 2020 are presented here to cover all 3 seasons of India. We have run the model for 80 h in forecasting mode for the reported period, and the model output used is forecast for the 3rd day (i.e. valid at 72 h).

Model Configuration: An accurate representation of physical, dynamical, chemical processes and their interaction at a fine-scale is important to the accurate predictions of meteorology and air quality. The use of nesting enables the simulation of feedbacks among various meteorological and chemical processes occurring at various temporal and spatial scales as shown in Fig. 3. Some studies have shown that using nested domains can lead to more accurate predictions of chemical species (Grell et al., 2005; Fast et al., 2006). The present system uses 2-way nesting which involves feedback from the fine domain to the coarse domain and vice versa. We have set 4 nested domains for each city. The grid resolution for outermost domain (1) is taken as 45 km × 45 km. It is considered as 15 km × 15 km for domain 2 and 5 km × 5 km for domain 3. The grid size of inner most domain (4) was 1.67 × 1.67 km. Two outermost domains (1 and 2) which cover parts of Europe and Asia (extends from −10.6°S 56.5°N in the north-south direction, and 31°E to 120°E in an east-west direction with 195 (W-E) x 173 (N–S) grid cells), and India (stretching from 55.4°E to 95°E (258 grid cells), and 2.7°N to 55.4°N (270 grid cells)) are common for SAFAR forecasting set-up of four cities. While the 3rd domain for Ahmedabad, Mumbai and Pune covers west India (300 × 324 grid cells in W-E and N–S direction), it covers North India (273 × 258 grid cells) for Delhi to take account of regional pollution from Indo-Gangetic Plain (IGP) region. The innermost domain (4) for Delhi, Ahmedabad, Mumbai and Pune contained 69 × 75, 69 × 75, 72 × 72, and 72 × 72 grid points in W-E and N–S direction. The centre latitude and longitude are 23.14°N, and 75.44°E respectively. The model projection is Mercator. The relaxation zones are within the grid point sizes, although grid point sizes are small. Total 32 vertical levels reaching to 50 hPa (as model top) have been used for all domains. Typically, 8–12 levels are there within boundary layer during day time. This can represent the vertical structure in daytime. The vertical resolution is 100 m for model vertical levels below 500 m, 200 m for model height in between 500 m-1Km; 500 m for model height between 1 and 3 km, and 1 Km for model height between 5 and 20 Km. This configuration works well as can be seen in our previous publications for non-rainy seasons (Chen et al., 2020; Srinivas et al., 2016; Beig et al., 2015). For monsoon season the vertical levels are increased for better vertical resolution of cloud related fields e.g. cloud water, water vapor etc. When there is high turbulence and vertical shear, overall vertical levels are increased to properly represent pollutant dispersion. The model has a lot of in-built physical parameterization options to choose from, although for a particular chemical scheme we cannot use every physics scheme. We have used the parameterization which showed optimal performance. Different physical parameterization used for set-up has been shown in Table S1. We have used CBMZ-MOSAIC 4-bin chemistry scheme consisting of Carbon Bond Mechanism version Z (CBMZ) gas-phase mechanism which contains 73 chemical species and 237 reactions, and MOSAIC (Model for Simulating Aerosol Interactions and Chemistry; Zaveri et al., 2008) aerosol scheme that uses 4 sectional bins where 3 bins are assigned for aerosols of diameter less than 2.5 μm, and other bin describing the size range 2.5–10 μm. The MOSAIC scheme describes the chemistry of sea salt (sodium, potassium, and chloride ions), soil (lumped inorganics), secondary inorganic aerosols (nitrate, sulphate, and ammonium ions), and carbonaceous aerosols (organic carbon and black carbon), and equilibrium between water vapor, 4 inorganic trace gases (NH_3, H_2SO_4, HNO_3, and HCl) with inorganic ions (nitrate, sulphate, and ammonium, and chloride).

Initial and boundary conditions: Long-range transport plays a key role on pollutant concentration along with emissions within the region. Therefore, to consider the influence outside the regions, lateral boundary conditions from the global model were used. The initial and boundary conditions for meteorological parameters are taken from NCEP-GFS (National Centre for Environmental Prediction -Global

Forecast System) discussed elsewhere (https://www.emc.ncep.noaa.gov/emc/pages/numerical_forecast_systems/gfs.php), which provides analyses and forecasts (available at 3 hourly intervals) with a global resolution of 0.25° × 0.25° to provide initial and boundary condition for meteorological parameters. Meteorological parameters include surface pressure, sea level pressure, geopotential height, temperature, sea surface temperature, soil temperature, soil water content, ice cover, relative humidity, u- and v-winds, vertical motion, vorticity and ozone profiles etc. The meteorological IC/BC is processed using WRF Pre-processing system (WPS) as shown in Fig. 3. The snow cover is processed from IC in our domains during model initialization using WPS. We have used model simulated chemical parameters from previous days run as the chemical initial condition for the next day. The boundary condition for gaseous and aerosol parameters was taken from WACCM (Whole Atmosphere Community Climate Model, https://www.acom.ucar.edu/waccm/download.shtml (Marsh et al., 2013 and references therein) with model output having a horizontal resolution 0.9° × 1.25° (https://www2.acom.ucar.edu/gcm/waccm) for 88 vertical levels available at 6 hourly intervals. The sea surface temperature is updated using SST data from the National Oceanic and Atmospheric Administration (https://polar.ncep.noaa.gov/sst/rtg_high_res/) at a resolution of 0.083° × 0.083°.

Meteorological Data and Forecasting: The ground level concentration of pollutants varies depending on the prevailing meteorological conditions at that time. Meteorological conditions are the prime factors that determine the dilution rate and dispersion of pollutants in the atmosphere. Therefore, meteorological data are essential for air quality forecasting. It aids in interpreting spatial and temporal variations of measured air quality data. They are also necessary inputs for dispersion model calculations of pollution concentrations. The chemical processes such as dust emission, fire emission, and biogenic emission are dependent on the simulated meteorological parameters such as vertical profiles of wind, temperature and relative humidity. At each scale, the land-use canopy and topographical effects are included to realize the regional synoptic meteorological conditions. For the finer scales, the urban canopy and anthropogenic heat island could also be introduced, if necessary. The final outputs for each domain are available at 1-h temporal resolution, with provision to only use the gridded fields for chemical transport modelling, but also to extract the data for either city grids (at a regional scale) and points of interest at finer resolutions (urban scale). The urban parameterization is an important aspect for megacities. Currently we are using default bulk parameterization for urban canopy in WRF-Chem. With detailed land use data at city level, we have the provision to use single layer urban canopy model. Cities are characterized by different physical properties of surface compared to their rural counterparts, resulting in a specific regime of the meteorological phenomenon. Hence, to assess the impact of cities on climate, inclusion of the urban parameterization is important in high resolution modelling as Halenka et al. (2019) have detected the urban heat island effect. Karlicky et al. (2018) have evaluated the impact of typical urban surfaces on the central European urban climate in several model simulations, performed with the WRF model and Regional Climate Model (RegCM) together with different descriptions of the urban environment. They have found that the urban environment improves the weather conditions a little with regard to the pollutant dispersion, which could lead to the partly decreased concentration of the primary pollutants, with the exception of the daytime in the summer. However, it may be stressed that only the concentration of primary pollutants can be decreased by urban effects and not the secondary pollutants that are created in the atmosphere (Huszár et al., 2018). However, from below 10 km, bulk schemes can reproduce parameters like urban heat island but are unlikely to resolve the mixing height or effects on wind at a finer resolution and likely to affect results. This is one of the weaknesses in the current model set-up.

Lin Microphysics which provides water/cloud variables in resolved scale has been used in the present framework. This scheme is well validated for cloud-permitting scale (5 Km) (Wang et al., 2009). Feedback from parameterized convection to the atmospheric radiation and the photolysis schemes is done in coupled (online) mode in the model in the resolved scale but not below 5 km. Feedback from the aerosols to the radiation schemes is allowed in all the scale. With use of UCM even at single level improve urban heat fluxes, evapotranspiration at high resolution city level. Additionally, we can use multi-layer urban canopy model e.g., BEP (which helps in getting vertically resolved wind and temperature fields), but due to high computational, and city level build, road etc. data requirement for multilayer UCMs, we do not use it in forecasting mode as done by most of other city scale forecasting models with a resolution in the order of 1 km or above. The UCMs incorporate the subgrid-scale physical processes of the urban environment using underlying heterogeneity of the urban surface. The required surface parameters are challenging to be defined properly and improper setting hinders model performance (Grimmond et al., 2011).

The Chemical Parameters: To simulate chemical parameters properly, we provided the latest anthropogenic emissions for gases (SO_2, NO_x, NH_3, CO, NMVOC), and aerosol species (BC, OC, $PM_{2.5}$, PM_{10}) from 5 sectors (residential biomass burning, power generation, small scale industry, transportation on land and water, for 3 outer domains from EDGAR-HTAP v4.3 (Crippa et al., 2018) at a resolution of 0.1° × 0.1°. We provided emission inventory for gases (SO_2, NO_x, CO, NMVOC) and aerosol species (BC, OC, $PM_{2.5}$, PM_{10}) for an additional sector of re-suspended road dust at city scale at a horizontal resolution of 1.67 × 1.67 km for the innermost domain for four cities prepared in our research group as mentioned earlier. We use utilities provided by UCAR/NCAR (https://www2.acom.ucar.edu/wrf-chem/wrf-chem-tools-community) along with some of the tools developed in collaboration during the inception of SAFAR framework in 2010 (Marappu et al., 2014). The emission for compounds from the biosphere is provided for each month using MEGAN v2.01 (Model of Emissions of Gases and Aerosols from Nature) which used a database for LAI and land cover (https://bai.ess.uci.edu/megan) and uses meteorological parameters such as solar radiation, temperature and moisture from WRF during runtime. The fire emissions during the stubble burning period in winter are taken from our recently developed dynamic emission inventory as discussed in detail elsewhere (Beig et al., 2020b). The fire emission for other period and regions were updated from Fire INventory from NCAR (FINN v1.5 (Wiedinmyer et al., 2011); which provides emissions of aerosols and gases using a fixed diurnal profile for fire emission, daily MODIS fire data at 1 Km x 1 Km resolution, vegetation data from satellite observation. To calculate the dry deposition, the parameterization of Wesely et al. (1989) is used to calculate surface resistance for gases and aerosols except for sulphate for which parameterization of Erisman et al. (1994) is used.

Challenges: The SAFAR faced number of challenges. To account the processes with varied geography and topography of a particular city was one of the major challenges in developing SAFAR framework. In general, open atmosphere that can be seen in central part of India is found to be favourable for the dispersion of pollutants. While Mumbai is blessed with sea on 3 sides which often send cleaner winds to balance city emission fury, Pune is located at higher altitude with greener cover and Ahmedabad is surrounded by open dry land. Open geography promotes diffusion of pollutants and hence air pollution emergencies are less likely to occur in those cities not walled up by obstacles. In contrast, Delhi is the landlocked city surrounded by unique geographical features likes Himalayas and the Thar desert. Because of extreme weather conditions in the region dispersion of pollutants becomes a major problem. Also, external transport of pollutants due to certain weather conditions is common feature in Delhi. Another challenge is accounting sources of air pollutants with unknown fluxes which are scattered around the city. Hence, to make the forecast accurate, one needs robust database of each and every air pollution source located in the city area and its geographical distribution over the region which is achieved to an extend but further high-resolution databases are always desirable. The Model Output Statistics (MOS) application enhanced operational forecast

ability of numerical model was a challenge which resulted in improving the accuracy for specific seasons (winter).

MOS Application to SAFAR Operational Forecast: To improve the skill and accuracy of forecast and to address the public information system adequately, SAFAR framework adopted the MOS application for the operational probabilistic forecasting (Andrés Pérez et al., 2015). Numerous studies have demonstrated the benefit of adjusting site-specific air quality model predictions using observational data to reduce systematic model bias (Miller et al., 2010). There are three reasons why statistical reinterpretation of dynamical numerical model output is useful for practical weather/air quality forecasting: (a) there are important differences between the real world and its representation in numerical models, (b) the numerical models are often not complete and true representations of the workings of the atmosphere, and their forecasts are subjected to errors and (c) the numerical models are deterministic where no randomness is involved in the development of future states of the system whereas practically the atmospheric environment do involve randomness. The MOS (Glahn and Lowry, 1972; Carter et al., 1989) is a type of statistical post-processing, a class of techniques used to improve numerical weather models' ability to forecast by relating model outputs to observational or additional model data (Dennstaedt, 2008; ECMWF, 2014 and Wilks, 2006) (https://www.weather.gov/mdl/mos_home). MOS is defined as an objective forecasting technique that consists of determining a statistical relationship between a predictant and variables forecast by a numerical model at some projection time. It is, in effect, the determination of the "weather/air pollutant related" statistics of a numerical model. Predictor points can come from either point observations or from data that has been calculated to points on a grid. The MOS products which are more heavily based on true observation points are referred to as station-based MOS, while MOS generated based on gridded data is called gridded MOS (GMOS) (Oosthuizen et al., 2020). The statistical method used in this work is multiple linear regression. Other techniques are possible, such as polynomial or logistic regression; or neural networks (Wilks, 2006) but we adopted the regression methodology due to its advantage with SAFAR kind of observational set-up as discussed above.

A general form of MOS equation can be written as below:

$$y = b_0 + b_1x_1 + b_2x_2 + b_3x_3 + \ldots \ldots b_nx_n \quad (1)$$

$$y_m = b_0 + b_1x_1 + b_2x_2 + b_3x_3 + \ldots \ldots b_nx_n \quad (2)$$

Where y denotes the predictand, here $PM_{2.5}$ and PM_{10} and x1 … … … xn denote predictors which are, forecasted meteorological parameters, b_0 expreses intercept and b1 …. bx are coefficients of predictors are used to improve forecast, y_m is a improved value obtained after applying regression equation.

3.5. Translating Data to information

The process of converting scientific data to useful application is very crucial and important as general public are usually not aware with the complex scientific data terminology or units. Hence the concept of Air Quality Index (AQI) is adapted by many countries (USEPA, 2005, 2014) to communicate pollution levels to common public in simplified and easy-to-understand format. In India, the initial work on the concept of Air Quality Index has been done by the SAFAR in 2010 (Beig et al., 2010). However, the official notification by Govt. of India on National Air Quality Index has been implemented in 2015 to strengthen air quality dissemination system for public awareness and to encourage involvement of common citizens in air quality management plans (MoEFCC, 2015). AQI is a rating scale used for reporting the quality of air we breathe in and the associated health effects. It provides information in terms of colour, and simple numbers without any units which can be easily understood by common public. There are six AQI categories namely Good, Satisfactory, Moderate, Poor, Very Poor and Severe as per official Indian government guidelines (MoEFCC, 2015). The breakpoint for the concentration for PM_{10} and $PM_{2.5}$ is given in Table 1.

3.6. Technological framework, data flow and outreach

The path from generating raw data to decisions that generates social and economic benefits is complex and needs scientific understanding and their linkages with socioeconomic aspects at each step. Hence, the most essential part of any early warning framework is to design a user-friendly system product and information dissemination tolls so that the information products generated through the system can be utilised by various stakeholders. This has improved awareness and helped in mitigation planning which is leading to achieve *"better city, better environment, better life"*. It will help to achieve faster, more inclusive and sustainable growth which we are committed by rendering services on air quality. SAFAR generates the following products and developed the following dissemination tools:

System Products: The SAFAR framework provides following information products:

1. AIR QUALITY: AQI based on location specific current and 3 days advance air quality forecast.
2. WEATHER: Location Specific current and 3 days advance weather Forecast.
3. EXTREME EVENTS: Alert for extreme pollution and weather events.
4. ADVISORIES: Advisories for human health and Skin.
5. EMISSION SCENARIO: To generate pollutant emission map at city level for mitigation.
6. HARMFUL RADIATION: Location Specific current UV-index Information at city level.

Information Dissemination: To disseminate the information related to SAFAR products, following tools are designed:

1. SAFAR-AIR- Mobile App: Available at google store and app stores.
2. SAFAR-INDIA: Dynamic web portal: Available at: http://safar.tropmet.res.in/
3. LED- Digital Display Board System for data screening
4. SAFAR-IVRS (Integrated Voice Response Service): Toll free Number
5. Registration for alert services through online and E-mail-safar@tropmet.res.in

All the activities of SAFAR from receiving data to dissemination are controlled by SAFAR-Master control centre (SMCC) located in IITM, Pune. It houses all important servers and prototype customised control software. It is equipped with high-tech service modules which facilitate online screening of data monitored at various locations in a city environment and online status of different equipment installed. The SMCC is also equipped with controls to remotely monitor the health of

Table 1
The concept of Air Quality Index (AQI) for India and breakpoints of PM_{10} and $PM_{2.5}$ for different categories with colour coding.

Description and Colour Coding	Air Quality Index (AQI) Range	PM_{10} (µg/m^3) 24 hr average	$PM_{2.5}$ (µg/m^3) 24 hr average
Good	0-50	0-50	0-30
Satisfactory	51-100	51-100	31-60
Moderate	101-200	101-250	61-90
Poor	201-300	251-350	91-120
Very Poor	301-400	351-430	121-250
Severe	401-500+	431+	250+

instruments, sensors, network communication, etc. The current and model forecasted data are translated to various products as stated above. The AQI is indicated via the different colour coding for the different categories. The data products thus generated are used for scientific research and development purposes as well for services to the society. Various products and dissemination tools like display boards, mobile-app, website etc are used for the data dissemination. For further detail reader is referred to visit SAFAR website (http://safar.tropmet.res.in).

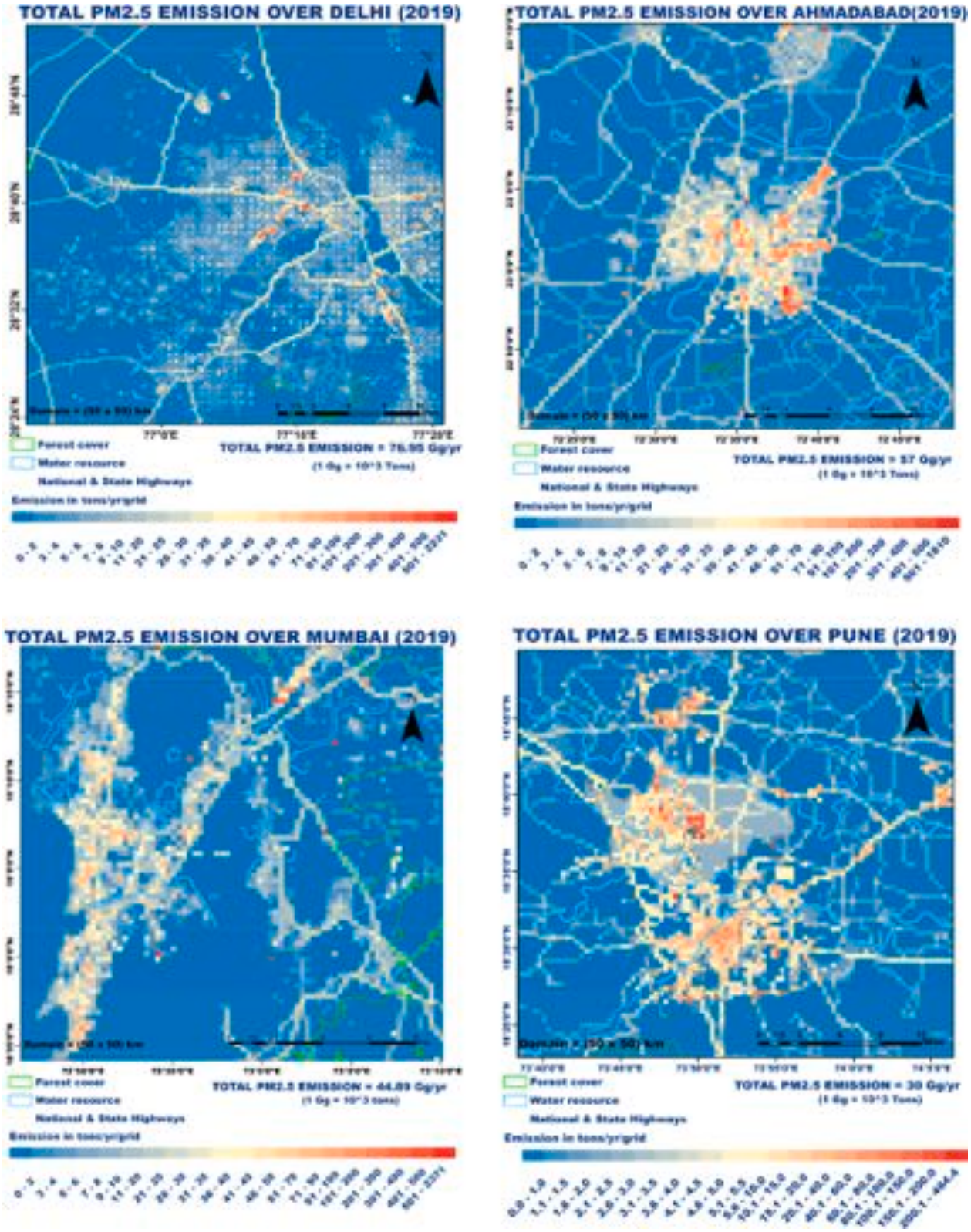

Fig. 4. The spatial distribution of total $PM_{2.5}$ emissions from all sources for Delhi, Mumbai, Ahmedabad and Pune in Tons/year for 1.67 × 1.67 km grid scale.

4. Results and model evaluation

4.1. Emissions of $PM_{2.5}$ and PM_{10}

The spatial distribution of $PM_{2.5}$ emissions from all sources is shown in Fig. 4. The estimated total emissions of $PM_{2.5}$ from all sources are calculated as 77 Gg/Year, 57 Gg/Year, 45 Gg/Year and 30 Gg/Year for geographical regions of Delhi, Ahmedabad, Mumbai and Pune metropolis respectively. It is observed from Fig. 4 that the trend of high emission $PM_{2.5}$ of the order of 200–1000 ton/yr is present over eastern, central, some part of the south-eastern region of Delhi which includes major roads network and industrial zones. Some industrial and slum related residential zones in Mumbai are the major point and area sources of $PM_{2.5}$ with the emission of the order of 200–2000 ton/yr/grid. A large number of $PM_{2.5}$ hotspots can be seen in central and eastern parts of Delhi, Pimpri Chinchwad Township in Pune and the South-South-east part of Ahmedabad due to industries and rising demand of the vehicle. However, the western and northern region of Delhi shows a comparatively lower value of $PM_{2.5}$ emission due to agricultural land cover and low population density being semi-urban zone. The oceanic regions in the Mumbai map are shown with blue colour with almost negligible emissions and hence not included in the inner most domain. However, they are accounted in outer domain. The relative contributions of different sectors (%) in different cities are shown in Fig. 5. High population density due to urbanization is the main reason which directly or indirectly drives the $PM_{2.5}$ emissions in all four metropolises. The most dominating emission source of $PM_{2.5}$ is transportation whose share is found to be 41% in Delhi followed by 40%, 35% and 31% in Pune, Ahmedabad and Mumbai respectively as shown in Fig. 5. All major traffic junctions are found to have high $PM_{2.5}$ emissions. The numbers of transport vehicles are rising rapidly in Delhi and Pune leading to congestion. Some load was reduced after implementation of Compressed Natural Gas (CNG) but the gain was offset by the rapid increase in the number of vehicles in recent times. Although, the share of the transport sector as compared to other sectors in Ahmedabad and Mumbai is also highest but due to the rapid bus transport system in Ahmedabad and local train services known as the lifeline of Mumbai has a significant impact in reducing the share of vehicular emissions. A large number of $PM_{2.5}$ hotspots are well scattered and can be identified in all cities due to the presence of industries as a point source and slum clusters as an area source. Uncontrolled combustion pattern in highly dense slum population in Mumbai is significantly high in Mumbai. The share of biofuel emissions is highest in Mumbai (15.5%) followed by Pune (11.4%), Ahmedabad (10.2%) and Delhi (3%). The industrial emissions mainly consist of emissions from the product and the fuel used in the unit.

The relative share is found to be highest (21.6%) in Pune, followed by Ahmedabad (18.8%), Delhi (18.6%) and Mumbai (31.1%). Emissions from power plants, mainly due to coal combustion are relatively less in all 4 cities. Low population density drives to limited combustion activities also. The sixth category of 'other sources' includes solid waste, trash burning, brick kiln, etc. which may individually appear to be very small but collectively, contribute a significant amount of $PM_{2.5}$ emission. Another major sector that contributes a significant amount of emissions of $PM_{2.5}$ is the emissions of re-suspended windblown dust from paved and unpaved roads and construction activities. The re-suspended dust is associated with the vehicular movement on the road and is directly proportional to the number of vehicles, its weight and speed as well as the amount of dust on roads. It is likely to be more serious in a city like Delhi, due to high vehicle numbers and in Ahmedabad, due to dry and hot weather. It has been found that windblown dust is not a major source of $PM_{2.5}$ and when compared to other sectors, it ranked 2nd in the list for Delhi and Ahmedabad but 3rd in Pune and 4th in Mumbai.

The spatial distributions of PM_{10} follows almost the same trend as $PM_{2.5}$ but with different magnitude and the relative share of different sectors in PM_{10} and the total emissions (Gg/Year) for each of the 4 cities are also shown in Fig. 5. The total aggregated emissions from all sources of PM_{10} are estimated as 177.9 Gg/Year, 90.7 Gg/Year, 84.6 Gg/Yr and 53.9 Gg/Year for Delhi, Ahmedabad, Mumbai and Pune respectively. The most dominating emission source of PM_{10} is found to be windblown resuspended dust whose share is found to be 46.4% in Delhi followed by 37.3%, 28.5% and 25.9% in Ahmedabad, Pune and Mumbai respectively as shown in Fig. 5. Vehicle movement over the major road network is the main source of windblown dust and confined to major downtown roads. The naturally blowing dust due to winds is a factor but in a heavily populated city like Delhi, it aggravates due to vehicle movements. The estimated windblown dust emission of PM_{10} is almost three times more than the transport sector emission. The uncertainty associated with road dust is assumed to be in largest and estimated to be more than 30% due to emission factors as well as the average weight of the vehicles traveling on the road mixed with prevailing winds which cannot be accurately determined as it is a dynamic and random process. Paved and unpaved road emissions are found to be lower over the outskirt of all cities as well as over some of the western and northern Delhi regions where the transport activity is limited. The relative share of industrial emissions in coarser particles, PM_{10}, are found to be significant (27.6%) in Ahmedabad as compared to similar source share in $PM_{2.5}$ because of the type of industries and unpaved road conditions transporting goods with a heavy load of resuspended dust.

4.2. Model validation

Model performance is evaluated using the daily averaged $PM_{2.5}$ observations at 4 monitoring cities in India: Delhi, Ahmedabad, Mumbai, and Pune for one year period (February 1, 2019 to January 31, 2020) covering all seasons. Fig. 6a and Fig. 6b show the verification of three days predicted temporal variations along with observations in the mass concentration of daily mean $PM_{2.5}$ and PM_{10} respectively during the above period at the four SAFAR cities. Each city consists of around 8–10 different locations. The red dots represent observed daily (24hr mean) mass concentrations data averaged over these 8–10 stations along with the range of values (minimum and maximum) in these different micro-environments, whereas continuous line (black) represent the model simulated 24hr averaged data of three days forecast for the identical period and grids. The deviation from the mean for model simulated data is not show for the sake of clarity. In Fig. 6a and b, some higher values are truncated by restricting the scale for better resolution and clarity but data are accounted in the analysis. In general, the predicted values are found to be in good agreement with observed data in all cities. The levels of PM_{10} and $PM_{2.5}$ were highest in Delhi followed by Ahmedabad, Mumbai, and Pune. The annual mean mass concentrations levels of PM_{10} and $PM_{2.5}$ were observed as 183 $\mu g/m^3$ and 93 $\mu g/m^3$ at Delhi, 120 $\mu g/m^3$ and 61 $\mu g/m^3$ at Ahmedabad, 96 $\mu g/m^3$ and 51 $\mu g/m^3$ at Mumbai and 70 $\mu g/m^3$ and 39 $\mu g/m^3$ at Pune, respectively during the study period. The mean concentrations for $PM_{2.5}$ in the summer season were 81 $\mu g/m^3$, 77 $\mu g/m^3$, 70 $\mu g/m^3$ and 42 $\mu g/m^3$ for Delhi, Ahmedabad, Mumbai, and Pune respectively. In monsoon, mean $PM_{2.5}$ levels were found to be 43 $\mu g/m^3$, 43 $\mu g/m^3$, 21 $\mu g/m^3$, 21 $\mu g/m^3$ and in winter they were 153 $\mu g/m^3$, 64 $\mu g/m^3$, 62 $\mu g/m^3$, 53 $\mu g/m^3$ for Delhi, Ahmedabad, Mumbai, and Pune respectively. Similarly, the average PM_{10} concentrations during summer season were 194 $\mu g/m^3$, 153 $\mu g/m^3$, 119 $\mu g/m^3$, 83 $\mu g/m^3$, in monsoon, 116 $\mu g/m^3$, 82 $\mu g/m^3$, 46 $\mu g/m^3$, 39 $\mu g/m^3$ and in winter 239 $\mu g/m^3$, 127 $\mu g/m^3$, 14 $\mu g/m^3$, 88.5 $\mu g/m^3$ for Delhi, Ahmedabad, Mumbai and Pune respectively. In the monsoon season, the particulate matter concentration is lowest as compared to the other seasons in all four cities due to the washout effect. The variability of particulate pollutants during monsoon is highly dependent on the number of rainy days and its intensity. The levels of these pollutants significantly dropped down in Pune and Mumbai which have recorded quite high rainfall activity during the monsoon season, spread around the entire season. The variability and trends in high concentration episodes of PM_{10} and $PM_{2.5}$ observed during extreme events were reasonably well captured by the model but often with significantly

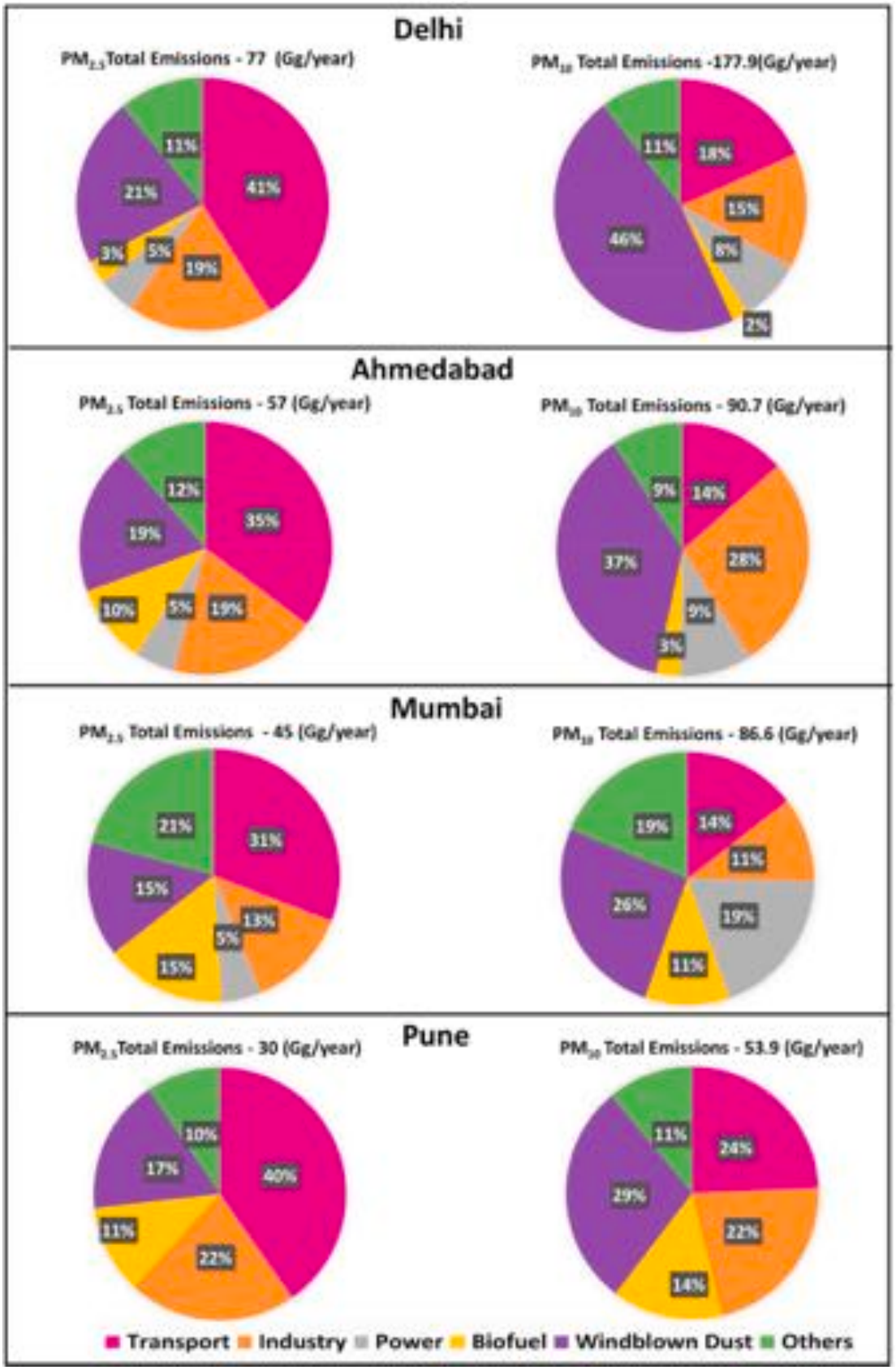

Fig. 5. Relative share of different source sectors in $PM_{2.5}$ and PM_{10} emissions (%) along with total $PM_{2.5}$ and PM_{10} emissions from all sources in Gg/year (written on top of each chart) for all 4 SAFAR cities considered in this work.

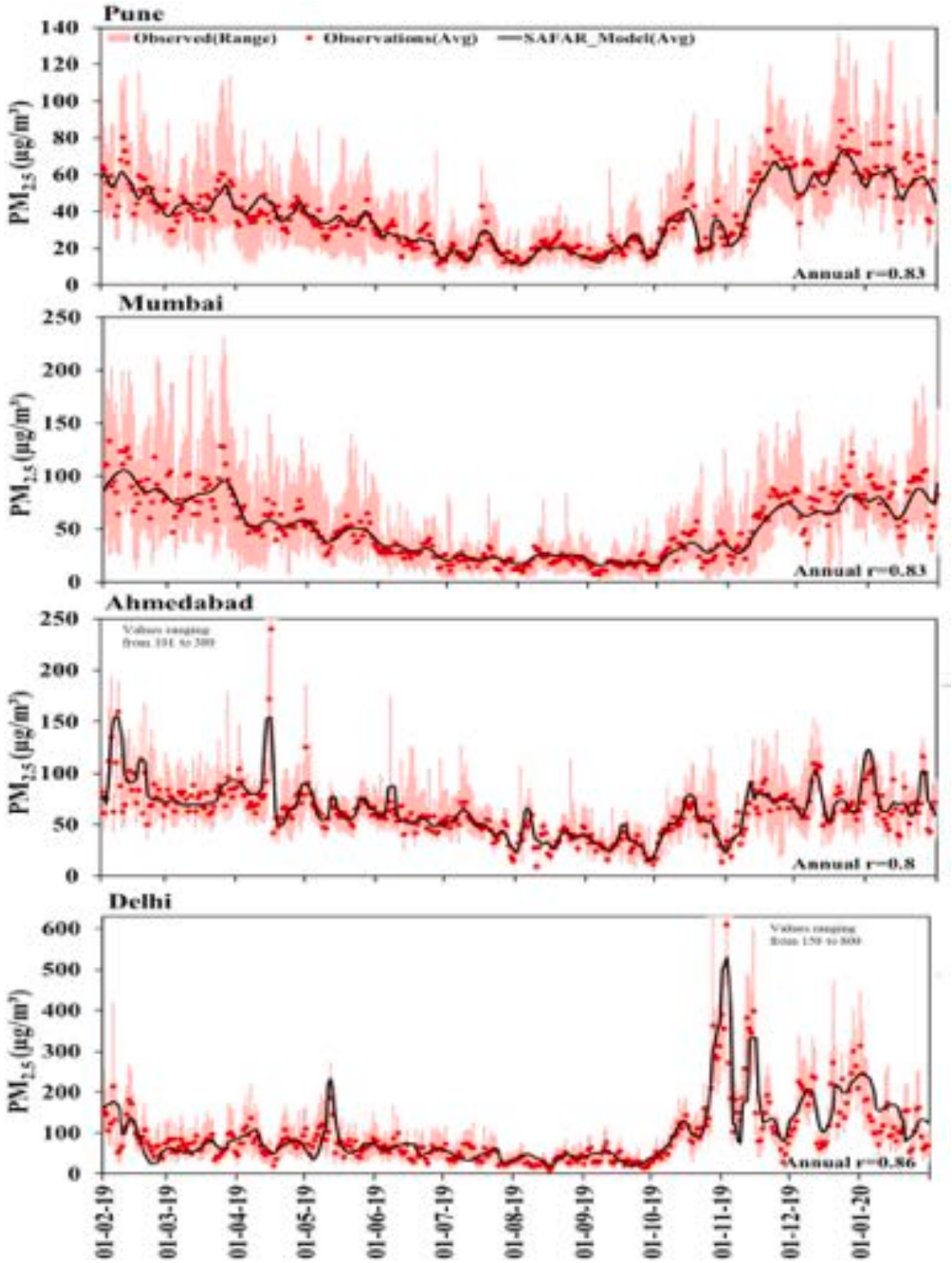

Fig. 6a. The time series of the verification of 3-days forecast of $PM_{2.5}$ daily averaged data (24hr average) for the period February 1, 2019 to 31st January' 2020 in Delhi, Ahmedabad, Mumbai and Pune. The observational data are represented with red dots (averaged over all 10 stations -mean) along with the range of values (min and max) from 10 stations. The model data of identical period and grid points are shown with continuous line (black) without showing the scatter to avoid overlap.

underestimated magnitude. This is one of the major shortcomings of the model for which a special treatment is worked out which will be discussed later in this paper. In case of a prolonged spell of an extreme event, the difference in predicted magnitude is high on initial days but later the error difference reduces, and skill of forecast improves significantly. In addition, the predicted surface winds during extreme events in winter are often found to be more intense than those observed, particularly in Delhi, leading to a more dilution of aerosol particles to under-estimate $PM_{2.5}$ levels.

The scatter plots for evaluation of the model performance in different seasons in terms of correlation coefficient are shown in Fig. 7a and 7b for PM2.5 and PM10 respectively. In general, correlation is found to be significant in all the seasons but with varying numbers. The correlation is found to be strongest for both $PM_{2.5}$ and PM_{10} during winter season in all 4 cities. It is relatively weak during monsoon season in Delhi due to erratic nature of rainfall.

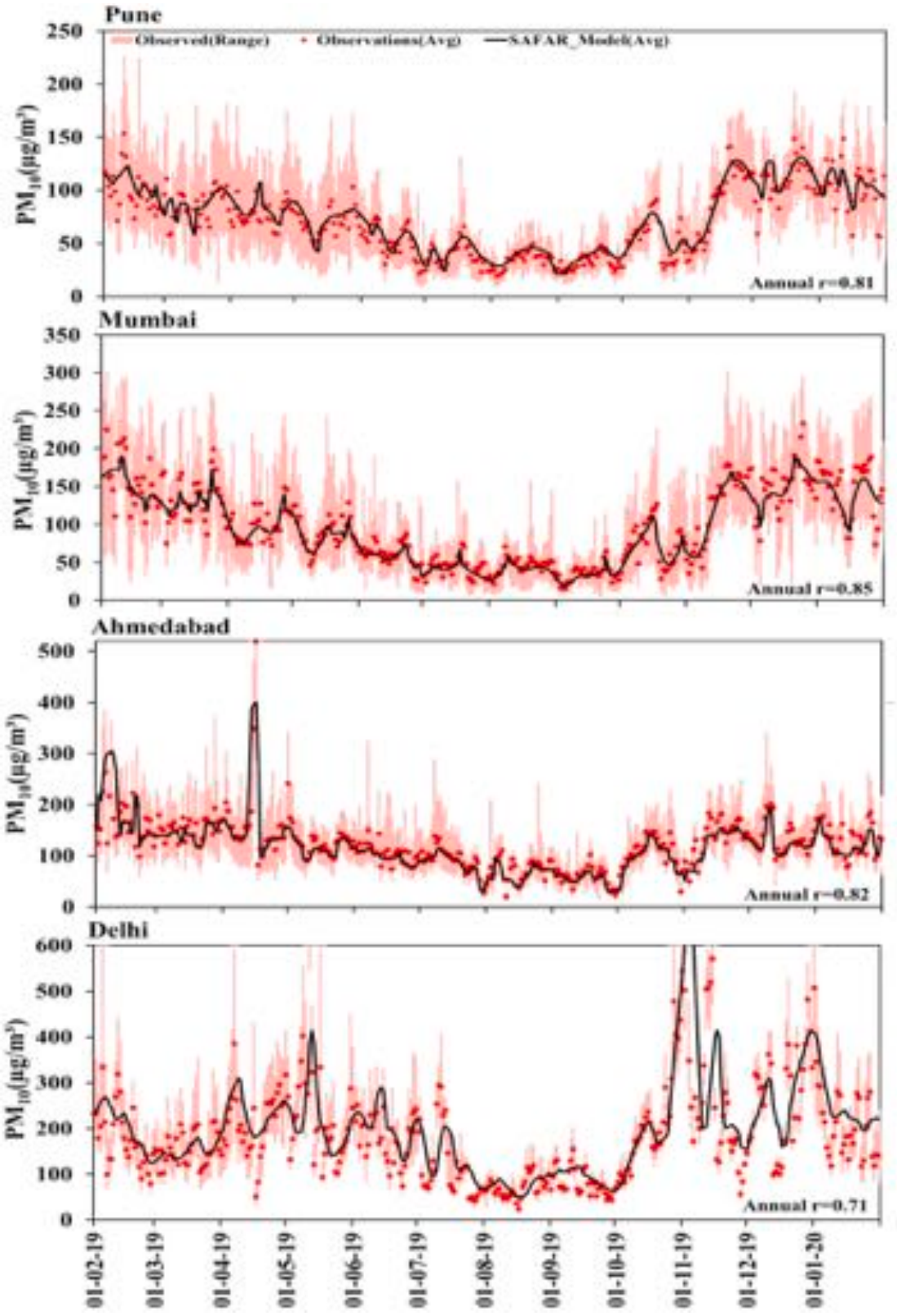

Fig. 6b. The time series of the verification of 3-days forecast of PM_{10} daily averaged data (24hr average) for the period February 1, 2019 to 31st January' 2020 in Delhi, Ahmedabad, Mumbai and Pune. The observational data are represented with red dots (averaged over all 10 stations -mean) along with the range of values (min and max) from 10 stations. The model data of identical period and grid points are shown with continuous line (black) without showing the scatter to avoid overlap.

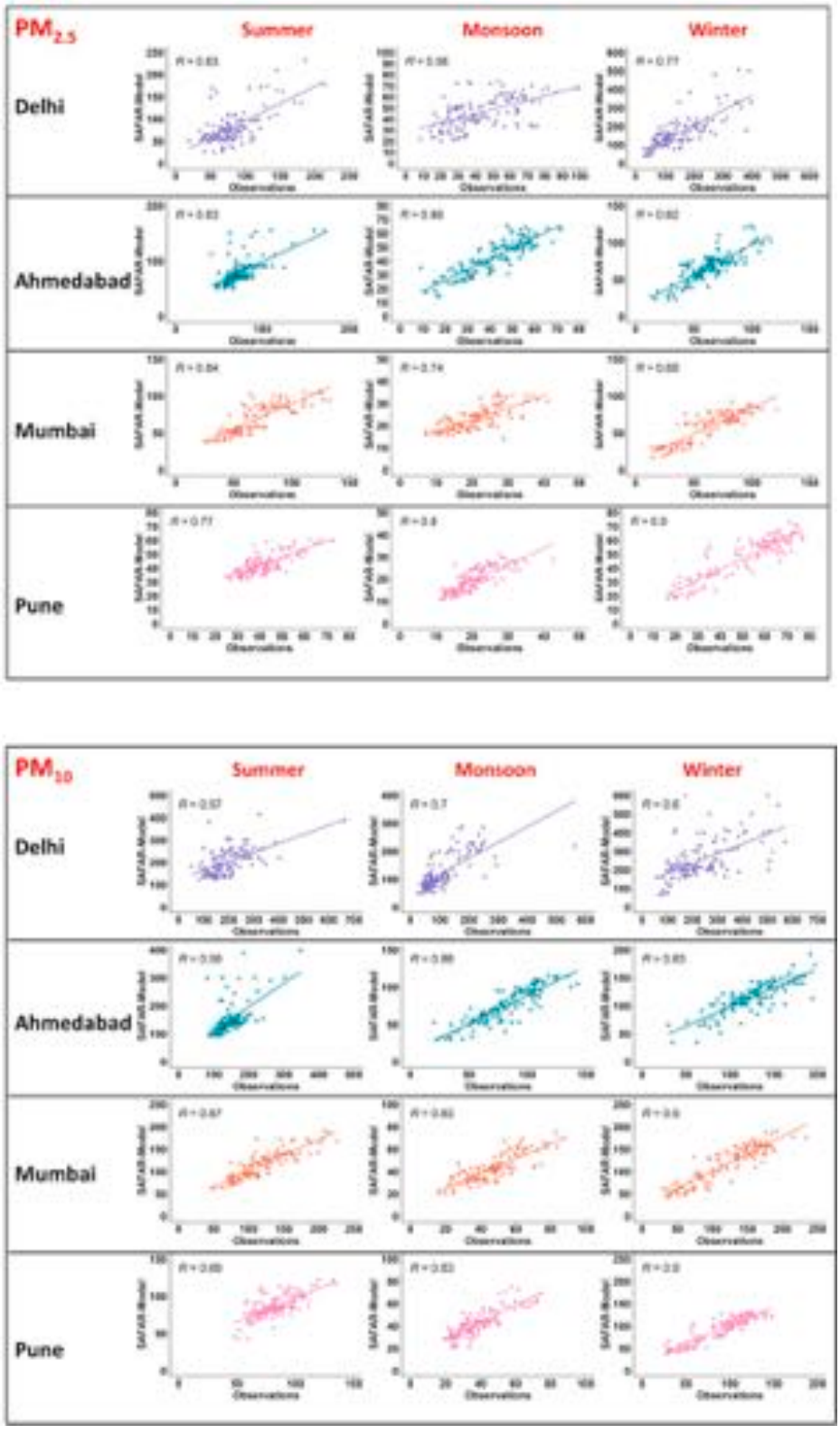

Fig. 7. The scatter plots for evaluation of the model performance in different seasons in terms of correlation coefficient for (a) PM2.5 and (b) PM10 in all 4 SAFAR cities.

The monthly averaged PM_{10} and $PM_{2.5}$ mass concentration as simulated by the online SAFAR forecasting model (red bars) with 3 days lead time in Delhi, Ahmedabad, Mumbai, and Pune are compared with observations (blue bars) in Fig. 8. The standard deviations from the mean across the ten SAFAR locations of each city are also shown.

On an average model performance is found to be reasonable. The scatter in the upper limit of PM_{10} and $PM_{2.5}$ in model output in different locations from October to February is found to be high as compared to observations, particularly for Delhi and during monsoon for Pune. In Ahmedabad, the concentration is found to be highest in the months of

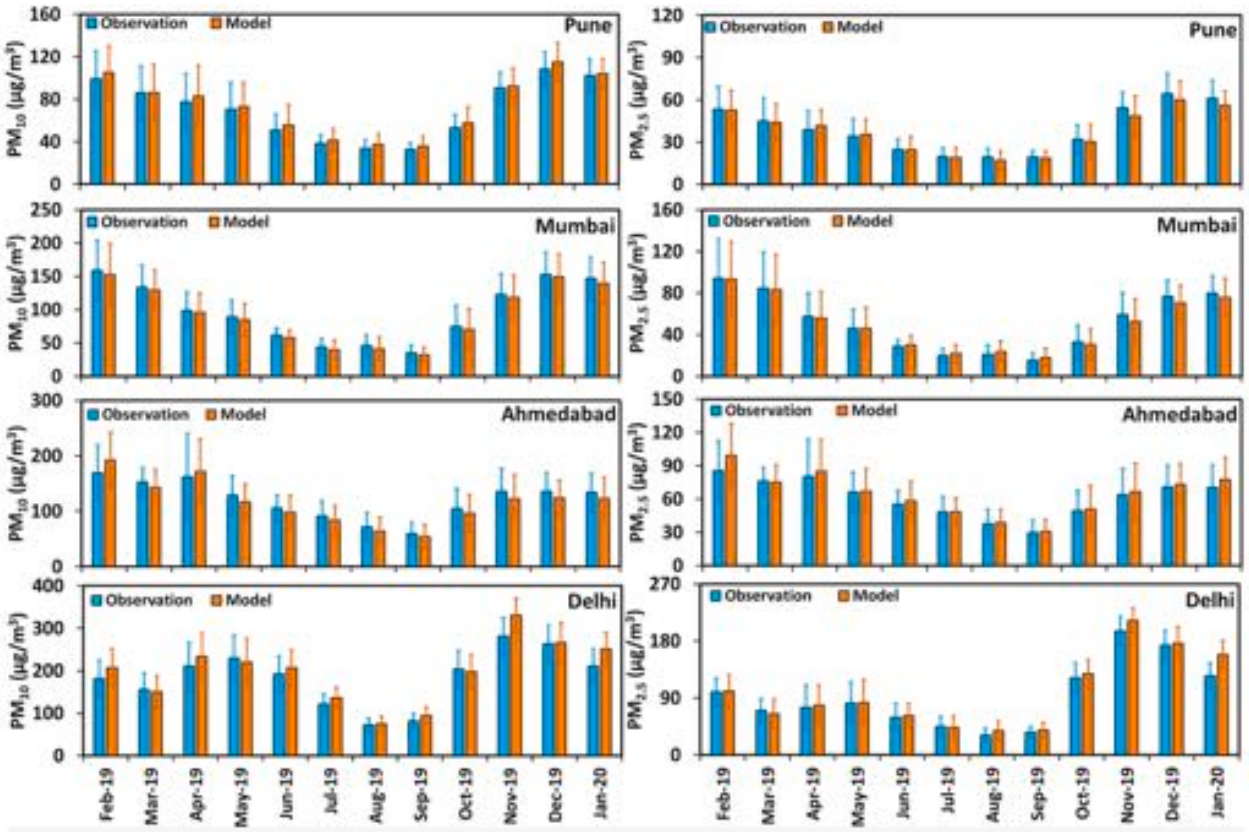

Fig. 8. The comparison of 3-day advance $PM_{2.5}$ and PM_{10} forecast averaged over each month as obtained from model and observations during the period February 1, 2019 to 31st January' 2020 in Delhi, Ahmedabad, Mumbai and Pune. The histogram is the monthly mean, averaged value over all 8–10 stations. The error bar shown in each histogram is the range of scatter in the monthly mean among all 8–10 stations.

February to April for both PM_{10} and $PM_{2.5}$. This is the time when the temperature is warmer and frequent episodes of local dust lifting takes place. Thus, it is observed that in Pune and Delhi, the levels of Particulate matter are higher in the winter season whereas in Mumbai, $PM_{2.5}$ concentration is highest at the onset of the summer season. Ahmedabad has the highest particulate matter concentration during the summer months as opposed to the winter season. This is mainly due to the high temperatures and frequent dust storms that occur in the summer season (Anand et al., 2019).

Fig. 9 shows the daily observed and predicted variability in surface

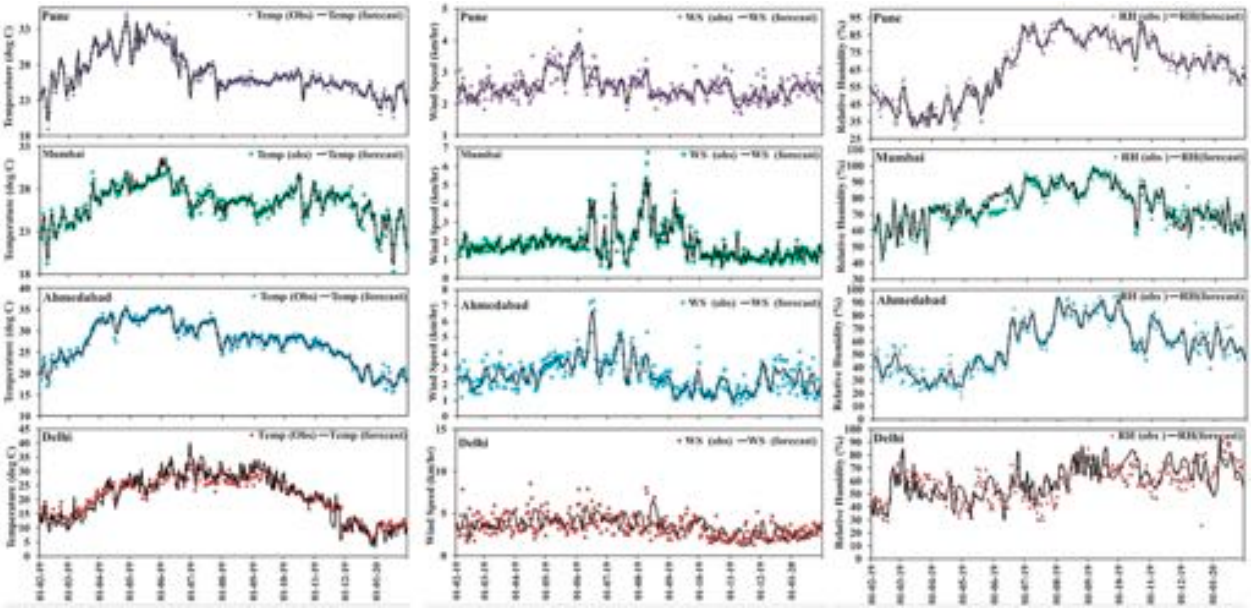

Fig. 9. The comparison of model forecasted value and observations of averaged temperature, wind speed and relative humidity of the day during the period February 1, 2019 to 31st January' 2020 in Delhi, Ahmedabad, Mumbai and Pune.

temperature, wind speed and relative humidity respectively at all four cities during the study period. The modeled meteorological parameters are broadly consistent with the observed daily temporal variability in all four cities. When we look at the temporal variability of temperature at the four cities it is observed that Delhi has the maximum variability in temperature ranging from 5 °C to 36 °C, whereas Mumbai showed the least variability in temperature with the temperature varying from 18 °C to 30 °C (Fig. 9). The wind speed observations showed seasonal variability in all cities except Delhi. Mumbai and Ahmedabad had higher wind speeds during the monsoon season, whereas Pune showed higher wind speed during the pre-monsoon period from May to June. In Delhi, the wind speed was lowest during winter as compared to the other seasons. Relative Humidity follows a common pattern in Pune and Ahmedabad with the peak (ranging from 70 to 95%) in relative humidity in Monsoon season which further extends to October–November months. In Mumbai, the relative humidity is higher as it is a coastal city (mostly above 50%) and during peak monsoon season it is mostly as high as 99%. It can be observed that in Delhi the relative humidity starts to increase from mid-July onwards as the onset of monsoon season here is comparatively late (in July) as compared to the other cities. Another relevant parameter for air quality is mixing layer height which has been validated for the whole year and found to be reasonably well simulated except during severe winter days which may likely to introduce some uncertainty in results as discussed later in this paper. This may be attributed to coarser resolution of bulk scheme for urban canopy.

4.3. Model skill and MOS application

To evaluate the SAFAR model's prediction skill against the measured PM_{10} and $PM_{2.5}$ mass concentrations, an extensive model performance evaluation was carried out to complement the qualitative graphical time series analysis (Fig. 6a and b). In this study, the statistical measures namely mean bias (MB), normalized mean bias (NMB), Mean Gross Error (MGE) and Mean Normalized Gross Error (MNGE) are used to assess model performance in simulating PM_{10}, $PM_{2.5}$ and meteorological variables. These metrics have been applied earlier in numerous studies for the estimation of regional air quality model performances (Feng et al., 2016; Sánchez-Ccoyllo et al., 2007). The MB captures the absolute bias in prediction with the positive and negative values represents the data from the dataset is either overestimated or underestimated, respectively, MGE measures the absolute error of model versus observation, NMB represents the normalization of MB and quantifies the model error by dividing by observed data mean and MNGE represents the mean absolute percentage error between the observed and predicted value relative to observed data. The mathematical equations to compute various statistical markers to evaluate the model performance are provided in the supplementary section (Statistical Parameters for Model evaluation).

The US Environmental Protection Agency (US-EPA, 2005) guideline states that the performance evaluations results would be acceptable when normalized bias and gross error statistics fall within the range (±) 5–15%, and 30–35%, respectively. Table 2 shows the performance evaluation result of the PM_{10} and $PM_{2.5}$ modelling. For the whole period, the normalized bias with SAFAR model forecast for PM_{10} is 20.7%, −2.7%, −1.7% and 9.5% and for $PM_{2.5}$, it is 16.5%, 8.5%, 6.3% and −1.3% in Delhi, Ahmedabad, Mumbai and Pune respectively, which indicate good performance for all cities except Delhi whose bias margin is slightly higher than the acceptable limit as prescribed by US-EPA (Table 2). The Normalized Gross error for Delhi is highest among all 4 cities for both PM_{10} (34.8%) and $PM_{2.5}$ (34.7%) during the whole period. Whereas for the other cities the normalized gross error during the whole period for both PM_{10} and $PM_{2.5}$ lies around 13–20%. The normalized gross error for Delhi is observed to be highest in the winter season for PM10 and monsoon season for $PM_{2.5}$ (Table 2). In Mumbai, the normalized gross error for $PM_{2.5}$ is highest in the monsoon season at 25% and for PM_{10} it is marginally higher in the winter season.

The normalized gross error (19.7%) of PM_{10} in Pune is higher during the monsoon season and for Ahmedabad, it is (17%) higher in the summer season. Thus, the normalized gross error is within the US-EPA acceptable limits for all the cities when the annual period is considered, however for Delhi it is just at the margin of acceptable limit during monsoon and winter season.

The monthly averaged PM_{10} and $PM_{2.5}$ mass concentration as simulated by the online SAFAR forecasting model with 3 days lead time in Delhi, Ahmedabad, Mumbai and Pune are compared with observations in Fig. 8. The standard deviations from the mean across the ten SAFAR locations of each city are also shown. The model output is shown

Table 2
Evaluation of SAFAR model performance and prediction skill against the daily averaged measured PM_{10} and $PM_{2.5}$ mass concentrations (Fig. 6a and b) for different seasons and annually in all 4 cities. The statistical measures, namely, mean bias (MB), normalized mean bias (NMB), Mean Gross Error (MGE) and Mean Normalized Gross Error (MNGE) are provided in the table.

	$PM_{2.5}$ (SAFAR-model v/s Observation)				PM_{10} (SAFAR-Model v/s Observation)			
	Pune	Mumbai	Ahm'bad	Delhi	Pune	Mumbai	Ahm'bad	Delhi
	Summer							
Bias	0.8	−1.5	0.8	0.5	3.7	−4.2	2.2	8.4
Normalized Bias (%)	4.3	1.2	9	6.4	6.3	−1.0	4	15.1
Gross error	5.3	10.2	5.3	23.0	10.3	14.3	25.6	50.0
Normalized Gross error (%)	13	14.7	17.1	31.5	13	11.9	17.0	30.3
Correlation	0.78	0.84	0.65	0.63	0.70	0.87	0.66	0.57
	Monsoon							
Bias	−1	2	−1	2.9	3.7	−5	−7	11.7
Normalized Bias (%)	−3.3	17.4	7.9	21	13.0	−6.5	−5.6	25
Gross error	2.8	4.2	2.8	12.4	6.7	7.2	9.9	35.3
Normalized Gross error (%)	13.1	25	17.1	36.8	19.7	16	13.1	36.3
Correlation	0.80	0.76	0.85	0.56	0.83	0.83	0.88	0.70
	Winter							
Bias	−4.1	−4.2	−4.1	15.1	3.8	−4.6	−10.5	21.7
Normalized Bias (%)	−4.8	1	8.6	22	9.3	1	−5.9	22
Gross error	7.1	10.2	7.1	45.1	11.0	18.0	15.4	75.8
Normalized Gross error (%)	14.1	19.6	17.1	35.7	16.3	17.4	12.8	37.8
Correlation	0.90	0.90	0.82	0.80	0.90	0.85	0.84	0.61
	Annual							
Bias	−1.4	−1.2	−1.4	6.2	3.7	−4.2	−5.1	14.0
Normalized Bias (%)	−1.3	6.3	8.5	16.5	9.5	−1.7	−2.7	20.7
Gross error	5.1	8.2	5.1	26.9	9.3	16.4	16.9	53.7
Normalized Gross error (%)	13.4	19.8	17.1	34.7	16.4	15.8	14.3	34.8
Correlation	0.83	0.83	0.83	0.9	0.81	0.85	0.82	0.7

as an orange bar whereas observational data are shown as blue bar. On an average model performance is found to be reasonable. The scatter in the upper limit of PM_{10} and $PM_{2.5}$ in model output in different locations from October to February is found to be high as compared to observations, particularly for Delhi and during monsoon for Pune. In Ahmedabad, the concentration is found to be highest in the months of February to April for both PM_{10} and $PM_{2.5}$. This is the time when the temperature is warmer and frequent episodes of local dust lifting takes place. Thus, it is observed that in Pune and Delhi, the levels of Particulate matter are higher in the winter season whereas in Mumbai, $PM_{2.5}$ concentration is highest at the onset of the summer season. Ahmedabad has the highest particulate matter concentration during the summer months as opposed to the winter season. This is mainly due to the high temperatures and frequent dust storms that occur in the summer season (Anand et al., 2019).

Table S4 shows the error analysis and its improvement when MOS methodology is applied to the model forecast. It is clearly depicted that MOS application marginal made some improvement in PM_{10} and $PM_{2.5}$ forecast annually. However, NMB and MNGE have indicated the improvement for PM_{10} and $PM_{2.5}$ in a few seasons. In Delhi, the normalized bias of PM_{10} and $PM_{2.5}$ is improved from 22.30% to 12.16% and 21.95%–16.97% respectively, in winter when Delhi's air quality deteriorates to a maximum and the season is marked by a majority of extreme events. The normalized bias in PM_{10} also improves in summer from 15.14% to 11.10%. Similarly, a normalized gross error has also shown little correction from 37.81% to 36.67% in winter only. MOS refinement (NMB) for Ahmedabad is found to be 8.97%–3.96% in summer for $PM_{2.5}$ and normalized gross error for PM_{10} has shown around 1-digit bias correction in summer. MOS improved NMB have been noticed only for $PM_{2.5}$ in Mumbai from 17.39% to 16.30% in monsoon season and 1.18% to −0.13% improvement in summer. Whereas, for Pune NMB for PM_{10} changed from 9.30% to −0.69% in winter season.

5. Discussion

It is interesting to note that the level of particulate pollution is significantly high during winter in Delhi and Pune but it is higher during summer in Ahmedabad as compared to other seasons. Unlike other cities, in Mumbai, the $PM_{2.5}$ levels are higher in summer but PM_{10} levels are higher in winter as compared to winter and summer respectively. This is mainly due to the fact that winter in Delhi and Pune are relatively cooler where boundary layer height and local meteorology plays a dominating role, particularly in Delhi where winter is severe.

In Delhi, calm wind conditions together with cooler temperature and low inversion layer adversely impact the air quality and keep particulate pollutants close to the surface. In addition, frequent episodes of radiative fog due to fall in local temperature with high humidity and advective fog originating from Indo-Gangetic plane regions along with westerly disturbances play a major role in deteriorating the air quality and keeping levels of particulate pollutants at elevated levels. In addition to this, the stubble burning in neighboring Northern states with favourable meteorology often leads to extreme pollution episodes in landlock Delhi. Ahmedabad is marked by mild winter but experiences severe summer when the temperature often crosses 40 °C leading to the local lifting of dust to elevate levels of coarser particulate matters. However, such dust lifting episodes as well as dust storms are common during summer in Delhi and Ahmedabad. The occasional peaks during the summer season in Delhi are mainly attributed to the migration of dust from desert regions of Rajasthan and surrounding regions under the warmer and dry season of summer (Anand et al., 2019). This is the main reason for the seasonal variability observed in these cities. The trends in dust storm-related extreme events during summer in Delhi as well as in Ahmedabad are well captured by the model but it often underestimates the magnitude. The SAFAR model has a choice of using any of the 2 schemes from Georgia Institute of Technology–Goddard Global Ozone Chemistry Aerosol Radiation and Transport (GOCART) and Air Force Weather Agency (AFWA). The GOCART and AFWA are two schemes uses different parametrization of dust emission as a function of wind and land parameters e.g. soil moisture, soil texture etc. We try to choose between GOCART and AFWA to get more realistic dust emission and to improve the skill of forecast based on the synoptic condition. The choice of using the scheme is decided on the nature of dust episodes by examining satellite image before the start of the model simulation during operational forecasting. Mumbai is a coastal city with high relative humidity. The variability in particulate pollutants is mainly driven by the land-ocean-land winds whereas seasonal variation in temperature from winter to summer is not very high.

The simulated concentrations are found to be generally over-estimated for $PM_{2.5}$ but under-estimated for PM_{10} when compared to measurements for Mumbai (Fig. 6). Mumbai often witnesses lows and high during winter and summer and significant variability from one location to another. This trend is due to the pattern of persistent local winds over the land area, causing the pollution loads from critical emission areas from one side to the other side. However reverse process follows when the coast of Mumbai induces the sea-breeze circulations and cleans the land area. Hence, under-prediction of PM_{10} could be associated with frequent wind reversal and faster deposition of coarser particles which are probably not simulated by the model as per the ever-changing real word situation. Although, wind considers the effect of local heating, the model resolution of 1.67 may not well represent the steep change in topography hence, the simulated $PM_{2.5}$ concentration is sometime over-estimated as it is associated with residential household emissions from Mumbai slums whose day to day variability may be exploited by abrupt change in local winds. The PM_{10} concentration in Delhi during the monsoon season shows that during the initial months of the season the concentration does not decrease significantly unlike other cities. This is attributed to the late arrival of south-west monsoon in Delhi as compared to the other 3 cities which are located in the western part of India, where the monsoon reaches quite early. However, the particulate matter concentration is lowest in this season in all 4 cities and the model simulation also captures this in all the cities with larger variability due to uncertainty in simulating the short-term rainfall fluctuations. During the study period considered, the rainfall extended even during October and November months in Mumbai and Pune due to which the particulate matter concentration was relatively lower. However, levels of PM start to increase from the beginning of November in these cities. Generally, the southwest monsoon withdraws from the North-west part of India by September end - October beginning but due to the cyclonic activity in the Arabian Sea during October and November months,' Mumbai and Pune received rainfall, thereby reducing the particulate matter concentration even in these months. The month to month variability in Delhi during winter months is mainly attributed due to the fact that air quality is highly vulnerable to short term variability in weather parameters during winter which is not well simulated by the model, particularly the mixing layer height and local wind speed. The rainfall in Pune is quite erratic during the monsoon season and changes its characteristics frequently in a short time span which might be one of the many reasons for the relatively weaker performance of the model in Pune during July to September. A sharp increase in the levels of PM_{10} and $PM_{2.5}$ is noticed in Delhi (Fig. 6) after September which is linked to the withdrawal of monsoon from Delhi in the first week of October. Immediately after the withdrawal of south-west monsoon, anticyclone establishment is one of the major synoptic features which make the whole atmosphere very stable due to air circulation associated with clear skies and sinking motion which forces stagnant conditions for quite some time (Beig et al., 2019). However, when such a condition starts to ease out, the temperature starts to drop faster in Delhi to bring down the mixing layer. At the same time, stubble burning in the Northern part of India often starts to push parcels of $PM_{2.5}$ towards Delhi based on boundary layer wind direction and speed and the air quality of Delhi starts to deteriorate rapidly (Beig et al., 2020b). The stubble

burning almost stops by the end of November but the air quality of Delhi continues to be highly affected even during December and January due to its land lock geography which plays an important role in trapping the pollutants during calm wind and cool conditions observed during these months (Hama et al., 2020; Anand et al., 2019). The cooler temperature brings down the atmospheric boundary layer further.

6. Conclusions

The air pollutant forecasting is an important part of the air quality early warning framework reported in this work for Indian megacities of vivid micro-environments. But the chaotic nature and complexity of the air pollution itself makes prediction a challenging task, particularly in a city which is highly influenced by meteorology due to its geographical location which are considered in this work. In this paper, the first official indigenous framework for India SAFAR is presented to forecast the concentration of particulate air pollutants which determines the air quality in Indian megacities with three days lead time as commited by SAFAR to India's National Clean Air Programme (NCAP) plan. Bias-variance and error evaluation systems were used to verify the stability and accuracy of the forecast. The results show that the SAFAR model has reasonably good accuracy and stability in predicting PM_{10} and $PM_{2.5}$ levels in contrasting micro-environments of Indian megacities and capture the trend of the data. The statistics verification analysis show that it predicts the extreme pollution event reasonably well but also over-estimates the concentrations of $PM_{2.5}$ and under-estimate PM_{10}. The potential weakness of the model system setting is related to usage of coarser bulk scheme for urban canopy which should be improved in the future to account for micro level urban processes connected to urban infrastructure. The application of MOS when applied to optimize the initial weights and thresholds, it reduces the impact of noise on the prediction results by retaining the actual trend of the data. However, the present model forecast is found to be quite robust and the application of the MOS methodology in air quality forecast in Indian metropolis improves the accuracy for some seasons which differ from city to city but do not make any significant change.

Author contribution

Anand, Bano, Rathod, Korhale, and Parkhi contributed in data curation, formal analysis and part writing and discussion. Sahu and Mangaraj contributed to emissions inventory, editing, and reviewing. Maji, Sobhana and Srinivas contributed towards software, model simulation and validation. Shinde contributed in development of outreach application and algorithms. Trimbake contributed in instrumentation. Peshin and Singh supervised the project data management and ensured the QA-QC. Beig (GB) as Project Director of SAFAR, contributed in conceptualization, paper writing and overall supervision.

Declaration of competing interest

The authors declare that they have no known competing financial interests or personal relationships that could have appeared to influence the work reported in this paper.

Acknowledgements

The authors acknowledge with thanks the Director (IITM) and Director General (IMD). Exclusive sense of indebtedness to Dr. (Mrs.) Parvinder Maini (MoES) for advancing SAFAR with probity. Special gratitude to Dr. Shailesh Nayak, Ex-Secretary, Ministry of Earth Sciences (Govt. of India) for his vision and confidence in GB to steer SAFAR and making it a flagship program of MoES. SAFAR fulfilled commitment to NCAP plan of Central Pollution Control Board of India. The funding for the research is from the core institutional (IITM) grant for SAFAR project sponsored by Ministry of Earth Sciences, India.

Appendix A. Supplementary data

Supplementary data to this article can be found online at https://doi.org/10.1016/j.envsoft.2021.105204.

References

Anand, V., Korhale, N., Rathod, A., Beig, G., 2019. On processes controlling fine particulate matters in four Indian megacities. Environ. Pollut. 254 https://doi.org/10.1016/j.envpol.2019.113026.

Andrade, Maria de Fatima, Ynoue, Rita Y., Dias, F.E., Enzo, T., Angel, V.V., Sergio, I., Droprinchinski, M.L., Alberto, M.J., Barreto, C.V.S., 2015. Air quality forecasting system for Southeastern Brazil. Front. Environ. Sci. 3, 1–14. https://doi.org/10.3389/fenvs.2015.00009.

Arora, P., Jain, S., Sachdeva, K., 2014. Physical characterization of particulate matter emitted from wood combustion in improved and traditional cookstoves. Energy for Sustainable Development 17, 497–503.

Balakrishnan, K., et al., 2019. The impact of air pollution on deaths, disease burden, and life expectancy across the states of India: the Global Burden of Disease Study 2017. Lancet Planet. Heal. 3, e26–e39. https://doi.org/10.1016/S2542-5196(18)30261-4.

Beig, G., Sahu, S.K., 2018. Safar High Resolution Emission Inventory of Megacity Delhi 2018. (Special Scientific Report; SAFAR-Delhi-2018-A, ISSN: 0252-1075). Ministry of Earth Sciences, Govt. of India.

Beig, Gufran, Ghude, S.D., Deshpande, A., August- 2010. Scientific Evolution of Air Quality Standards and Defining Air Quality Index for India, *ISSN0252-1075, IITM, Research Report No-Rr127*.

Beig, G., Chate, D.M., Sahu, S.K., Parkhi, N.S., Srinivas, R., Ali, K., Ghude, S.D., Yadav, S., Trimbake, H.K., 2015. System of Air Quality Forecasting and Research (SAFAR-INDIA). GAW Report No. 217. World Meteorological Organization, Global Atmosphere Watch, Geneva, Switzerland.

Beig, G., Srinivas, R., Parkhi, N.S., Carmichael, G.R., Singh, S., Sahu, S.K., Rathod, A., Maji, S., 2019. Anatomy of the winter 2017 air quality emergency in Delhi. Sci. Total Environ. 681, 305–311. https://doi.org/10.1016/j.scitotenv.2019.04.347.

Beig, G., George, M.P., Sahu, S.K., Rathod, A., Singh, S., Dole, S., Murthy, B.S., Latha, R., Tikle, S., Trimbake, H.K., Shinde, R., 2020a. Towards baseline air pollution under COVID-19: implication for chronic health and policy research for Delhi, India. Curr. Sci. 119.

Beig, G., Sahu, S.K., Singh, V., Tikle, S., Sobhana, S.B., Gargeva, P., Ramakrishna, K., Rathod, A., Murthy, B.S., 2020b. Objective evaluation of stubble emission of North India and quantifying its impact on air quality of Delhi. Sci. Total Environ. 709, 136126. https://doi.org/10.1016/j.scitotenv.2019.136126.

Bieringer, P.E., Longmore, S., Bieberbach, G., Rodriguez, L.M., Copeland, J., Hannan, J., 2013. A method for targeting air samplers for facility monitoring in an urban environment. Atmos. Environ. 80, 1–12. https://doi.org/10.1016/j.atmosenv.2013.06.012.

Carter, G., Dallavalle y J Glahn, H., 1989. «Statistical Forecasts Based on the National Meteorological Center's Numerical Weather Prediction System. » Weather and Forecasting, pp. 401–412.

Chen, Y., Wild, O., Ryan, E., Sahu, S.K., Lowe, D., Archer-Nicholls, S., Wang, Y., McFiggans, G., Ansari, T., Singh, V., Sokhi, R.S., Archibald, A., Beig, Gufran, 2020. Mitigation of $PM_{2.5}$ and ozone pollution in Delhi: a sensitivity study during the pre-monsoon period. Atmos. Chem. Phys. 20, 499–514. https://doi.org/10.5194/acp-20-499-2020.

Crippa, M., Guizzardi, D., Muntean, M., Schaaf, E., Dentener, F., Van Aardenne, J.A., Monni, S., Doering, U., Olivier, J.G.J., Pagliari, V., Janssens-Maenhout, G., 2018. Gridded emissions of air pollutants for the period 1970-2012 within EDGAR v4.3.2. Earth Syst. Sci. Data 10. https://doi.org/10.5194/essd-10-1987-2018, 1987–2013.

Dennstaedt, S., 2008. Model output statistics provide essential data for small airports. The Front. NOAA's National Weather Service 6 (2), 1–11. Volume 6, Number 2," NOAA's National Weather Service.

ECMWF (European Centre for Medium-range Weather Forecasting), 2014. The MOS Equation. www.ecmwf.int/products/forecasts/guide/The_MOS_equation.html. (Accessed December 2014). accessed.

Erisman, J.W., van Pul, A., Wyers, P., 1994. Parameterization of surface resistance for the quantification of atmospheric deposition of acidifying pollutants and ozone. Atmos. Environ. 28, 2595–2607.

Fast, J.D., Gustafson, W.I., Easter, R.C., Zaveri, R.A., Barnard, J.C., Chapman, E.G., Grell, G.A., Peckham, S.E., 2006. Evolution of ozone, particulates, and aerosol direct radiative forcing in the vicinity of Houston using a fully coupled meteorology-chemistry-aerosol model. J. Geophys. Res. Atmos. 111, 1–29. https://doi.org/10.1029/2005JD006721.

Feng, T., Li, G., Cao, J., Bei, N., Shen, Z., Zhou, W., Liu, S., Zhang, T., Wang, Y., Tie, X., Molina, L.T., 2016. Simulations of organic aerosol concentrations during springtime in the Guanzhong basin, China. Atmos. Chem. Phys. Discuss. 1–38. https://doi.org/10.5194/acp-2016-224.

Filonchyk, M., Hurynovich, V., 2020. Spatial distribution and temporal variation of atmospheric pollution in the South Gobi Desert, China, during 2016–2019. Environ. Sci. Pollut. Res. 27, 26579–26593. https://doi.org/10.1007/s11356-020-09000-y.

Gao, M., Carmichael, G.R., Wang, Y., Saide, P.E., Yu, M., Xin, J., Liu, Z., Wang, Z., 2016. Modeling study of the 2010 regional haze event in the North China Plain. Atmos. Chem. Phys. 16, 1673–1691. https://doi.org/10.5194/acp-16-1673-2016.

Glahn, H., Lowry, D., 1972. The use of model Output statistics (MOS) in objetive weather forecasting. J. Appl. Meteorol. 1203–1211.

Grell, G.A., Peckham, S.E., Schmitz, R., McKeen, S.A., Frost, G., Skamarock, W.C., Eder, B., 2005. Fully coupled "online" chemistry within the WRF model. Atmos. Environ. 39, 6957–6975. https://doi.org/10.1016/j.atmosenv.2005.04.027.

Grimmond, C.S.B., Blackett, M., Best, M., Baik, J.-J., Belcher, S., Beringer, J., Bohnenstengel, S., Calmet, I., Chen, F., Coutts, A., Dandou, A., Fortuniak, K., Gouvea, M., Hamdi, R., Hendry, M., Kanda, M., Kawai, T., Kawamoto, Y., Kondo, H., Krayenhoff, E., Lee, S.-H., Loridan, T., Martilli, A., Masson, V., Miao, S., Oleson, K., Ooka, R., Pigeon, G., Porson, A., Ryu, Y.-H., Salamanca, F., Steeneveld, G., Tombrou, M., Voogt, J., Young, D., Zhang, N., 2011. Initial results from Phase 2 of the international urban energy balance model comparison. Int. J. Climatol. 31, 244–272.

Grimmond, S., et al., 2014. Technical Report: "Establishing Integrated Weather, Climate, Water and Related Environmental Services for Megacities and Large Urban Complexes –Initial Guidance", Global Framework for Climate Services (GFCS). World Meteorological Organization (United Nations).

Gurjar, B.R., Aardenne, J.A.V., Lelieveld, J., Mohan, M., 2004. Emission estimates and trends (1990–2000) for megacity Delhi and implications. Atmos. Environ. 38 (33) https://doi.org/10.1016/j.atmosenv.2004.05.057, 5663- 568.

Halenka, T., Belda, M., Huszar, P., Karlicky, J., Novakova, T., Zak, M., 2019. On the comparison of urban canopy effects parameterisation. Int. J. Environ. Pollut. 65 (1–3), 177–194. https://doi.org/10.1504/IJEP.2019.101840. Special Issue.

Hama, S.M.L., Kumar, P., Harrison, R.M., Bloss, W.J., Khare, M., Mishra, S., Namdeo, A., Sokhi, R., Goodman, P., Sharma, C., 2020. Four-year assessment of ambient particulate matter and trace gases in the Delhi-NCR region of India. Sustain. Cities Soc. 54, 102003. https://doi.org/10.1016/j.scs.2019.102003.

Huang, Y., Yam, Y.S., Lee, C.K.C., Organ, B., Zhou, J.L., Surawski, N.C., Chan, E.F.C., Hong, G., 2018. Tackling nitric oxide emissions from dominant diesel vehicle models using on-road remote sensing technology. Environ. Pollut. 243, 1177–1185. https://doi.org/10.1016/j.envpol.2018.09.088.

Huszár, P., Karlický, J., Belda, M., Halenka, T., Pišoft, P., 2018. The impact of urban canopy meteorological forcing on summer photochemistry. Atmos. Environ. 176, 209–228. https://doi.org/10.1016/j.atmosenv.2017.12.037.

Karlicky, J., Huszar, P., Halenka, T., Belda, M., Zak, M., Pisoft, P., Miksovsky, J., 2018. Multi-model comparison of urban heat island modelling approaches. Atmos. Chem. Phys. 18, 10655–10674. https://doi.org/10.5194/acp-18-10655-2018.

Ma, C., Wang, T., Zang, Z., Li, Z., 2018. Comparisons of three-dimensional variational data assimilation and model output statistics in improving atmospheric chemistry forecasts. Adv. Atmos. Sci. 35, 813–825. https://doi.org/10.1007/s00376-017-7179-y.

Marrapu, P., Cheng, Y., Beig, Gufran, Sahu, S., Srinivas, R., Carmichael, G.R., 2014. Air quality in Delhi during the commonwealth Games. Atmos. Chem. Phys. 14, 10025–10059. https://doi.org/10.5194/acpd-14-10025-2014.

Marsh, D.R., Mills, M.J., Kinnison, D.E., Lamarque, J.F., Calvo, N., Polvani, L.M., 2013. Climate change from 1850 to 2005 simulated in CESM1(WACCM). J. Clim. 26, 7372–7391. https://doi.org/10.1175/JCLI-D-12-00558.1.

Miller, et al., 2010. In: AQMOS: Air Quality Model Output Statistics from CMAQ Model Forecast. Presented at the 9th Annual CMAS Conference. Chapel Hill, NC.

MoEFCC, Central Pollution Control Board, 2015. National Air Quality Index Report. https://app.cpcbccr.com/ccr_docs/FINAL-REPORT_AQI_.pdf.

Oosthuizen, C., van Wyk, B., Hamam, Y., Desai, D., Alayli, Y., 2020. The use of gridded model output statistics (GMOS) in energy forecasting of a solar car. Energies 13. https://doi.org/10.3390/en13081984.

Pérez, V., Arasa, R., Codina, B., Piñón, J., 2015. Enhancing air quality forecasts over catalonia (Spain) using model output statistics. J. Geosci. Environ. Protect. 3, 9–22. https://doi.org/10.4236/gep.2015.38002.

Placet, M., Mann, C.O., Gilbert, R.O., Niefer, M.J., 2000. Emissions of ozone precursors from stationary sources: a critical review. Atmos. Environ. 34, 2183–2204. https://doi.org/10.1016/S1352-2310(99)00464-1.

Powers, J.G., Klemp, J.B., Skamarock, W.C., Davis, C.A., Dudhia, J., Gill, D.O., Coen, J.L., Gochis, D.J., Ahmadov, R., Peckham, S.E., Grell, G.A., Michalakes, J., Trahan, S., Benjamin, S.G., Alexander, C.R., Dimego, G.J., Wang, W., Schwartz, C.S., Romine, G. S., Liu, Z., Snyder, C., Chen, F., Barlage, M.J., Yu, W., Duda, M.G., 2017. The weather research and forecasting model: overview, system efforts, and future directions. Bull. Am. Meteorol. Soc. 98, 1717–1737. https://doi.org/10.1175/BAMS-D-15-00308.1.

Rundell, K.W., 2012. Effect of air pollution on athlete health and performance. Br. J. Sports Med. 22267572. https://doi.org/10.1136/bjsports-2011-090823.

Sahu, S.K., Beig, G., Parkhi, N.S., 2011. Emissions inventory of anthropogenic PM2.5 and PM10 in Delhi during commonwealth Games 2010. Atmos. Environ. 45, 6180–6190. https://doi.org/10.1016/j.atmosenv.2011.08.014.

Sahu, S.K., Beig, G., Parkhi, N., 2015. High resolution emission inventory of NOx and CO for megacity Delhi, India. Aerosol Air Qual. Res. https://doi.org/10.4209/aaqr.2014.07.0132.

Sahu, S.K., Ohara, T., Beig, G., 2017. The role of coal technology in redefining India's climate change agents and other pollutants. Environ. Res. Lett. 12 https://doi.org/10.1088/1748-9326/aa814a.

Saikawa, E., Kim, H., Zhong, M., Avramov, A., Zhao, Y., Janssens-Maenhout, G., Kurokawa, J.I., Klimont, Z., Wagner, F., Naik, V., Horowitz, L.W., Zhang, Q., 2017. Comparison of emissions inventories of anthropogenic air pollutants and greenhouse gases in China. Atmos. Chem. Phys. 17, 6393–6421. https://doi.org/10.5194/acp-17-6393-2017.

Sánchez-Ccoyllo, O.R., Martins, L.D., Ynoue, R.Y., Andrade, M. de F., 2007. The impact on tropospheric ozone formation on the implementation of a program for mobile emissions control: a case study in São Paulo, Brazil. Environ. Fluid Mech. 7, 95–119. https://doi.org/10.1007/s10652-007-9018-7.

Schell, B., Ackermann, I.J., Hass, H., Binkowski, F.S., Ebel, A., 2001. Modeling the formation of secondary organic aerosol within a comprehensive air quality model system. J. Geophys. Res. Atmos. 106, 28275–28293. https://doi.org/10.1029/2001JD000384.

Seinfeld, J.H., Pandis, S.N., 2006. In: Atmospheric Chemistry and Physics: from Air Pollution to Climate Change, second ed. John Wiley & Sons, New York.

Shephard, R.J., 1984. Athletic performance and urban air pollution. Can. Med. Assoc. J. 131 (2), 105–109.

Smith, K.R., Uma, R., Kishore, V.V.N., Lata, K., Joshi, V., Zhang, J., et al., 2000. Greenhouse Gases from Small-Scale Combustion Devices in Developing Countries: Phase IIA, Household Stoves in India. U.S. EPA EPA/600/R-00/052. https://nepis.epa.gov/Exe/ZyPDF.cgi/P1009BSZ.PDF?Dockey=P1009BSZ.PDF.

Srinivas, R., Panicker, A.S., Parkhi, N.S., Peshin, S.K., Beig, G., 2016. Sensitivity of online coupled model to extreme pollution event over a megacity Delhi. Atmos. Pollut. Res. 7, 25–30. https://doi.org/10.1016/j.apr.2015.07.001.

Struzewska, Joanna, Kaminski, Jacek, Jefimow, Maciej, 2016. Application of model output statistics to the GEM-AQ high resolution air quality forecast. Atmos. Res. 181, 186–199. https://doi.org/10.1016/j.atmosres.2016.06.012.

UN report, 2016. The world's cities in 2016. https://www.un.org/en/development/desa/population/publications/pdf/urbanization/the_worlds_cities_in_2016_data_booklet.pdf.

US EPA (US Environmental Protection Agency), 2005. Guidance on the Use of Models and Other Analyses in Attainment Demonstrations for the 8-hour Ozone NAAQS. EPA-454/R-05–002. accessed in Juanuary 2018. http://www.epa.gov/scram001/.

USEPA (US Environmental Protection Agency), 2014. Air Quality Index. https://www.epa.gov/sites/production/files/2014-05/documents/zell-aqi.pdf.

Vara-Vela, A., Andrade, M.F., Kumar, P., Ynoue, R.Y., Muñoz, A.G., 2016. Impact of vehicular emissions on the formation of fine particles in the Sao Paulo Metropolitan Area: a numerical study with the WRF-Chem model. Atmos. Chem. Phys. 16, 777–797. https://doi.org/10.5194/acp-16-777-2016.

Wang, Y., Long, C.N., Leung, L.R., Dudhia, J., McFarlane, S.A., Mather, J.H., Ghan, S.J., Liu, X., 2009. Evaluating regional cloud-permitting simulations of the WRF model for the tropical warm pool international cloud experiment (TWP-ICE), Darwin, 2006. J. Geophys. Res.: Atmosphere 114 (D21).

Wesely, M.L., 1989. Parametrization of surface resistances to gaseous dry deposition in regional-scale numerical models. Atmos. Environ. 23, 1293–1304.

Wiedinmyer, C., Akagi, S.K., Yokelson, R.J., Emmons, L.K., Al-Saadi, J.A., Orlando, J.J., Soja, A.J., 2011. The Fire INventory from NCAR (FINN): a high resolution global model to estimate the emissions from open burning. Geosci. Model Dev. (GMD) 4, 625–641. https://doi.org/10.5194/gmd-4-625-2011.

Wilks, D.S., Wilks, D.S., 2006. In: Statistical Methods in the Atmospheric Sciences. International Geophysics, vol. 100. Academic Press.

Yadav, R., Sahu, L.K., Beig, G., Tripathi, N., Jaaffrey, S.N.A., 2017. Ambient particulate matter and carbon monoxide at an urban site of India: influence of anthropogenic emissions and dust storms. Environ. Pollut. 225, 291–303. https://doi.org/10.1016/j.envpol.2017.01.038.

Yadav, R., Sahu, L.K., Tripathi, N., Pal, D., Beig, G., Jaaffrey, S.N.A., 2019. Investigation of emission characteristics of NMVOCs over urban site of western India. Environ. Pollut. 252, 245–255. https://doi.org/10.1016/j.envpol.2019.05.089.

Zaveri, R.A., Easter, R.C., Fast, J.D., Peters, L.K., 2008. Model for simulating aerosol interactions and chemistry (MOSAIC). J. Geophys. Res. Atmos. 113, 1–29. https://doi.org/10.1029/2007JD008782.

SUPPLEMENTARY MATERIAL

INDIA'S MAIDEN AIR QUALITY FORECASTING FRAMEWORK FOR MEGACITIES OF DIVERGENT ENVIRONMENTS: THE SAFAR-PROJECT

Gufran Beig[a,*], S. K. Sahu[b], V. Anand[a,c], S. Bano[a], S. Maji[a], A. Rathod[a], N. Korhale[a,c], S. B. Sobhana[a], N. Parkhi[a], P. Mangaraj[b], R. Srinivas[a], S.K. Peshin[d], S. Singh[d], R. Shinde[a], and H.K. Trimbake[a]

[a] Indian Institute of Tropical Meteorology, Pune (Ministry of Earth Sciences), India.

[b] Utkal University, Bhubaneshwar.

[c] Savitribai Phule Pune University, Pune

[d] Indian Meteorological Department, New Delhi

*Corresponding Author; Email: beig@tropmet.res.in

Table S1: *Description of different physical and chemical parameterisation used in WRF-Chem based SAFAR-Air Quality Forecasting model framework.*

Parameterisation	Scheme used	Short Description
Radiation		
Longwave radiation	RRTM Longwave Scheme (Mlawer et al., 1997)	Solves the radiative transfer equation for upward and downward fluxes; accounts for multiple bands, trace gases; cloud –radiation feedback for cloud water, rain water, ice, snow, and graupel.
Shortwave radiation	Goddard Shortwave Scheme (Chou et al., 1994)	Two-stream multi-band scheme; uses stratospheric (upper level) ozone from climatology; AOD from chemistry module; Scattering effect of aerosols; cloud radiation feedback for cloud water and ice.
Boundary Layer		

Boundary Layer	Yonsei University Scheme (YSU) (Hong et al., 2006)	Diagnostic non-local approach: Uses non-local K approach to find the gradient of mass and momentum; PBL top/height is function of buoyancy profile; Explicit treatment of entrainment layer based on results from large-eddy simulations.
Land Surface	Unified Noah Land Surface Model (Tewari et al., 2004)	Predicts soil temperature and moisture, snow cover, frozen soil water, and provides sensible and latent heat flux to PBL scheme.
Surface Layer	Revised MM5 Scheme (Jimenez et al., 2012)	Use similarity theory to calculate exchange coefficients (for land surface models) and diagnostic of 2m temperature, moisture, 10m wind, and frictional velocity for PBL scheme.
Cloud		
Cloud Microphysics	Purdue Lin Scheme (Chen et al., 2002)	This model includes six classes of hydrometeors: water vapor, cloud water, cloud ice, rain, snow, and graupel, and assumes the hydrometeor population (mixing ratio or number density) distribution using some functional form.
Cumulus Parameterization	Grell–Freitas Ensemble Scheme (Grell and Freitas, 2014)	Used for domain 1 and 2 in our study; use ensemble of triggers (when to start convection) and closures; uses mass-flux based approach shallow convection.
Emissions		
Anthropogenic Emissions	SAFAR Emission Inventory & EDGAR v4.3.2	SAFAR inventory at 1.67km * 1.67 km resolution, EDGAR v4.3.2 (0.1° x 0.1°) Intercontinental Chemical Transport Experiment B (INTEX-B) data at 0.5°*0.5° resolution (Zhang et al., 2009).
Biogenic Emissions	MEGAN	MEGAN Model of Emissions of Gases and Aerosols from Nature, biogenic emissions online based upon the weather, land use data.
Fire Emissions	SAFAR and FINN	Stubble emission in North India (Beig et al., 2020) and FINN v1.5; Wiedinmyer et al., 2011

1. Statistical Analysis for Model evaluation

The mathematical equations governing various statistical parameters to evaluate the model performance are given below:

Mean Bias (MB)

$$\text{MB} = 1/n \sum_{i=1}^{n} (Mi - Oi) \quad \text{..... (1)}$$

Normalized Mean Bias (NMB)

$$\text{NMB} = 1/n \sum_{1}^{n} (Mi - Oi / Oi) \text{ x100} \quad \text{.....(2)}$$

Mean Gross Error (MGE)

$$\text{MGE} = 1/n \sum_{i=1}^{n} |(Mi - Oi)| \quad \text{.....(3)}$$

Mean Normalized Gross Error (MNGE)

$$\text{MNGE} = 1/n \sum_{1}^{n} (|Mi - Oi| / Oi) \text{x100} \quad \text{.....(4)}$$

Where, *Mi, Oi* and *n* are model output, observed values and sample count respectively (Feng et al., 2016).

Table S2 shows the bias of the model on a monthly scale for PM_{10} and $PM_{2.5}$. It is observed that the NMB is higher in Delhi as compared to the other cities. Mumbai has the lowest NMB for PM_{10} for all the months considered in this study. In Mumbai and Pune, the NMB is higher during the months of June to September for PM_{10} and $PM_{2.5}$. The NMB in Ahmedabad for PM_{10} is higher in the months of February and April and for $PM_{2.5}$ it is observed to be higher even in January. The NMB in Delhi is observed to be highest in Delhi in the months October and July for PM_{10} and for $PM_{2.5}$ it is highest in January and August. In Pune, the NMB is within the acceptable range according to the US-EPA performance results which is ±5-15 %. In

Mumbai, the NMB is higher than the acceptable range for $PM_{2.5}$ during the months of July to September. It is observed that in Ahmedabad the NMB in February is about 18% and 22% for PM_{10} and $PM_{2.5}$ which is higher than the US-EPA standard value. In Delhi the monthly NMB is on the higher side indicating that the model performing is relatively weaker. It is observed that the PM_{10} and $PM_{2.5}$ concentration is well simulated in Pune, Mumbai and Ahmedabad for all the months considered in this study in online mode. However, in Delhi we observe that when the concentration is higher the normalized mean bias is higher.

PM_{10}																			
	Pune				Mumbai				Ahmedabad				Delhi						
	MB	NMB	GE	MN	MB	NMB	GE	MN	MB	NMB	GE	MN	MB	NMB	GE	MN	MB	NMB	GE	MN
Feb-	6.09	8.89	13.2	14.44	-5.76	-0.88	20.41	12.92	22.88	17.84	44.36	29.19	25.74	25.25	51.4	34.62				
Mar-	0.66	3.2	11.01	14.24	-4.07	0.47	17.04	13.3	-9.7	-5.2	16.68	10.53	-5.16	1.5	29.08	19.4				
Apr-	5.74	9	9.55	13.08	-3	-1.14	11.23	10.95	9.37	11.01	31	21.15	24.44	24.79	48.35	33.12				
May-	2.55	4.34	7.78	11.38	-4.13	-2.43	9.15	10.33	-11.4	-7.48	12.47	8.57	-9.03	10.33	71.07	34.62				
Jun-	4.7	15.28	10.17	24.19	-3.43	-2.1	7.59	13.67	-7.24	-5.51	10.24	9.27	15.09	19.12	51.07	29.19				
Jul-19	3.14	11.24	5.89	17.57	-4.03	-3.93	9.04	20.52	-7.45	-6.9	9.19	10.07	15.38	39.84	49.06	53.87				
Aug-	3.48	12.57	5.28	17.6	-4.71	-8.06	6.47	13.64	-7.72	-4.53	12.33	19.67	3.46	13.78	18.29	28.71				
Sep-	3.51	12.8	5.62	19.54	-2.81	-4.25	5.71	16.28	-5.01	-5.44	7.98	13.39	13.19	25.53	22.8	32.94				
Oct-	4.78	18.83	10.49	26.57	-3.99	1.5	13.56	20.98	-7.6	-4.1	12.38	14.34	-5.54	-1.75	24.65	11.73				
Nov-	2	4.23	7.96	10.26	-4.04	1.08	12.57	13.94	-12.9	-7.75	18.39	14.71	49.09	47.32	147.7	69.15				
Dec-	6.65	8.37	12.31	12.89	-3.22	0.32	18.38	12.46	-10.8	-6.62	13.01	8.73	3.71	14.41	63.55	31.78				
Jan-	1.68	5.61	13.04	15.2	-6.98	-0.64	21.12	15.76	-10.5	-5.21	17.96	13.44	40.56	30.04	69.46	39.6				
$PM_{2.5}$																				
	Pune				Mumbai				Ahmedabad				Delhi						
	MB	NMB	GE	MN	MB	NMB	GE	MN	MB	NMB	GE	MN	MB	NMB	GE	MN	MB	NMB	GE	MN
Feb-	43.05	34.1	6.89	1.46	28.63	20.7	21.92	14.15	15.86	14.34	2.56	-1.2	12.68	6.57	1.78	-0.4				
Mar-	21.97	14.12	-0.81	-4.78	11.14	8.45	0.2	-0.52	16.97	13.64	2.9	-1.31	13.17	5.65	0.56	-0.85				
Apr-	24.49	14.81	13.49	3.59	21.57	16.49	12.21	4.95	12.23	7.15	0.32	-1.23	14.19	5.28	8.55	2.75				
May-	37.33	29.97	6.36	2.04	8.39	5.64	2.92	1.02	13.05	5.54	3.37	0.12	12	3.9	6.17	1.49				
Jun-	29.17	13.64	14.79	2.79	13.71	7.59	6.33	3.19	20.18	4.97	11.76	2.1	15.05	3.5	3.43	-0.16				
Jul-19	32.18	13.65	9.63	-1.42	11.98	4.69	4.3	0.31	27.85	4.34	20.04	2.16	11.93	2.57	-2.31	-0.77				
Aug-	44.05	9.81	37.78	7.2	26.75	7.26	13.77	1.61	21.86	3.96	17.5	2.6	12.38	2.59	-	-2.34				
Sep-	41.68	12.48	21.5	3.02	15.95	4.1	7.32	1.45	32.42	3.82	27.07	2.54	12.9	2.44	-3.01	-0.56				
Oct-	15.78	18.14	8.13	6.28	14.81	6.01	5.81	1.59	27.54	8.01	1.91	-2.49	14.91	4.79	-0.48	-1.48				
Nov-	46.71	70.19	24.71	16.82	18.61	9.54	7.89	2.6	18.01	9.38	-6.02	-6.74	13.62	6.89	-9.8	-5.8				
Dec-	28.62	40	13.74	3.61	11.72	8.06	5.22	2.34	16.31	12.02	-3.81	-6.16	10.8	6.8	-4.86	-4.17				
Jan-	52.23	52.99	41.32	33.8	23.41	14.12	15.51	7.55	19.71	14.2	0.39	-3.99	17.2	9.95	-4.27	-4.92				

Table -S2: *Evaluation of model performance and prediction skill of monthly averaged value computed from 3-day advance daily forecast against the measured PM_{10} and $PM_{2.5}$ mass concentrations (Figure S1) for different seasons and annually in all 4 cities. The statistical measures namely mean bias (MB), normalized mean bias (NMB), Mean Gross Error (MGE) and Mean Normalized Gross Error (MNGE) are provided in the table.*

Table S3 shows the performance evaluation of the model simulated meteorological variables on a seasonal and annual scale on a daily averaged basis in terms of the statistical measures described above. During the whole period of the study, the normalized bias for temperature indicates a negative bias at all the four cities, with the lowest bias is estimated in Mumbai (-1) and it varies from 0 to -2.5 to -3 in the remaining other cities. This indicates good performance of the model. The model simulated temperature is well reproduced in all the four cities. However, when we look at the wind speed, the normalized bias is higher in all the four cities as shown in Table S3. The normalized bias for the whole period (annual scale) is large (Table S3) at all the four locations, which indicates the wind speed is overestimated by the model that is one of the major reasons for poor performance, especially during the winter period when calm winds tend to trap the pollutants in a landlocked city like Delhi. Delhi has the largest bias of 57% and in the winter season, the bias is largest thus the model overestimates the wind speed in Delhi to a larger extent. Relative humidity is well simulated in Pune and Mumbai which have an annual Normalized Bias of 0.6% and 0.2% respectively. In Ahmedabad the relative humidity has a normalized bias of -10% during the whole period of the study which is the largest with respect to the other cities, thus for Ahmedabad, the relative humidity is underestimated. The normalized gross error for the meteorological parameters indicates that it is highest for all the three parameters under consideration at Delhi on the annual scale as compared to the other cities. For wind speed, the normalized gross error at Delhi was highest at 70.9 % for the whole period of the study and in winter it was highest as compared to the other seasons at 90.8%. The normalized gross error for the temperature annually at Ahmedabad, Mumbai and Pune is 6.7, 2.5 and 4.5 respectively (Table S3). The normalized gross error in all cities is higher for the wind speed as compared to the other modeled meteorological parameters. Thus, it indicates that wind speed is overestimated in all cities.

SAFAR-Model v/s Observation: Meteorological Fields			Summer				Monsoon				Winter			
			Pun	Mum	Ahm	Del	Pun	Mum	Ahm	Del	Pun	Mum	Ahm	Del
Temperature	MB		-0.2	-0.2	-0.2	-1.1	-0.03	-0.7	-0.7	-0.7	-0.9	-1.1	-1.1	-1.1
	NMB		0.3	-1.0	-0.8	-7.1	-2.9	-2.5	-0.9	-2.5	-8.4	-1.9	-0.7	-4.5
	MGE		1.4	1.4	1.4	2.0	1.9	1.2	1.2	1.2	1.5	1.2	1.2	1.2
	NMGE		1.7	2.4	6.4	11.3	10.1	6.7	2.5	4.5	11.8	7.2	3.0	4.8
	CC		0.85	0.94	0.91	0.96	0.97	0.92	0.93	0.90	0.95	0.64	0.91	0.85
Wind Speed	MB		-0.2	-0.2	-0.2	1.7	1.6	-0.7	-0.7	-0.7	1.8	-1.1	-1.1	-1.1
	NMB		12.8	11.1	6.4	49.4	57	18.4	15.8	7.7	82.2	33.9	14.7	3.1
	MGE		1.4	1.4	1.4	2.3	2.2	1.2	1.2	1.2	2	1.2	1.2	1.2
	NMGE		16.5	13.6	21.1	64.0	70.9	31	22.2	12.9	90.8	46.4	22.2	9.9
	CC		0.58	0.68	0.64	0.41	0.42	0.91	0.80	0.93	0.20	0.31	0.41	0.56
Relative Humidity	MB		-0.2	-0.2	-0.2	-2.6	1	-0.7	-0.7	-0.7	1.9	-1.1	-1.1	-1.1
	NMB		2.8	0.5	-10.0	-2.3	3.7	-10	0.2	0.6	4.8	-10	1.7	0.08
	MGE		1.4	1.4	1.4	8.7	8	1.2	1.2	1.2	8.4	1.2	1.2	1.2
	NMGE		13.9	8.9	10.0	17.2	14.8	10	7.5	8.7	13.5	10	8.9	6.2
	CC		0.34	0.56	0.60	0.57	0.71	0.91	0.80	0.93	0.44	0.78	0.70	0.77

Table S3: *Evaluation of model performance and prediction skill against the daily averaged measured temperature, wind speed and relative humidity on sessional and annual scale for all 4 cities. The statistical measures namely mean bias (MB), normalized mean bias (NMB), Mean Gross Error (MGE) and Mean Normalized Gross Error (MNGE) are provided in the table. (Pun – Pune, Mum – Mumbai, Ahm – Ahmedabad, Del – Delhi).*

	$PM_{2.5}$ (MOS-MLR Model v/s Observation)				PM_{10} (MOS-MLR model v/s Observations)			
	Pune	Mumbai	Ahm'bad	Delhi	Pune	Mumbai	Ahm'bad	Delhi
	Summer							
Bias	2.8	-3.4	-1.2	4.9	4.1	1.6	-2.7	-3.4
Normalized Bias	8.2	-0.1	4.0	16.0	7.2	5.6	3.8	11.1
Gross error	10.1	13.7	13.7	25.0	16.9	19.7	27.1	61.7
Normalized Gross error	25.0	21.1	16.6	34.5	21.5	19.2	16.3	35.5
Correlation	0.5	0.7	0.3	0.4	0.5	0.8	0.3	0.3
	Monsoon							
Bias	4.6	2.5	0.9	14.1	6.6	2.8	2.7	18.2
Normalized Bias	27.4	16.3	12.2	53.9	24.2	10.4	12.2	42.2
Gross error	6.0	6.9	7.8	25.0	10.1	12.5	15.1	55.0
Normalized Gross error	32.2	35.2	24.5	76.7	30.4	29.9	24.0	63.0
Correlation	0.5	0.5	0.7	0.3	0.6	0.6	0.7	0.5
	Winter							
Bias	-7.4	0.9	0.2	-12.5	-10.6	-4.3	0.0	-14.8
Normalized Bias	-4.1	17.4	9.8	17.0	-0.7	8.9	6.9	12.2
Gross error	13.1	15.4	14.4	59.9	21.8	28.6	26.3	81.0
Normalized Gross error	26.4	33.6	25.9	43.3	27.7	28.4	23.2	36.7
Correlation	0.7	0.7	0.4	0.5	0.7	0.7	0.4	0.5
	Annual							
Bias	0.0	0.0	0.0	2.1	0.0	0.0	0.0	0.0
Normalized Bias	10.5	11.3	8.7	29.0	10.2	8.3	7.6	21.8
Gross error	9.7	12.0	12.0	36.8	16.3	20.3	22.8	66.0
Normalized Gross error	27.8	30.0	22.4	51.6	26.6	25.9	21.2	45.1
Correlation	0.7	0.8	0.7	0.7	0.8	0.9	0.7	0.6

Table S4*: Evaluation of the performance of MOS-MLR application to SAFAR operational forecast with observations. The statistical measures namely mean bias (MB), normalized mean bias (NMB), Mean Gross Error (MGE) and Mean Normalized Gross Error (MNGE) are provided in the table.*